

1 **Forecasting regional-level COVID-19 hospitalisation in England as an ordinal variable**
2 **using the machine learning method**

3 Haowei Wang^{1,2}, Kin On Kwok^{3,4,5}, Ruiyun Li⁶, Steven Riley^{1,2*}

4 ¹ School of Public Health, Imperial College London, UK

5 ² MRC Centre for Global Infectious Disease Analysis and Abdul Latif Jameel Institute
6 for Disease and Emergency Analytics, Imperial College London, UK

7 ³ JC School of Public Health and Primary Care, The Chinese University of Hong Kong,
8 Hong Kong Special Administrative Regions, China

9 ⁴ Stanley Ho Centre for Emerging Infectious Diseases, The Chinese University of
10 Hong Kong, Hong Kong Special Administrative Region, China

11 ⁵ Hong Kong Institute of Asia-Pacific Studies, The Chinese University of Hong Kong,
12 Hong Kong Special Administrative Region, China

13 ⁶ School of Public Health, Nanjing Medical University, 101 Longmian AV., Nanjing, Jiangsu,
14 211166, China

15 *Corresponding authors: Steven Riley, s.riley@imperial.ac.uk, School of Public Health,
16 Imperial College London, Norfolk Place, London, W2 1PG

17

18 Abstract

19 *Background*

20 COVID-19 causes substantial pressure on healthcare, with many healthcare systems now
21 needing to prepare for and mitigate the consequences of surges in demand caused by
22 multiple overlapping waves of infections. Therefore, public health agencies and health
23 system managers also now benefit from short-term forecasts for respiratory infections that
24 allow them to manage services better. However, the availability of easily implemented
25 effective tools for generating precise forecasts at the individual regional level still needs to be
26 improved.

27 *Methods*

28 We extended prior work on influenza to forecast regional COVID-19 hospitalisations in
29 England for the period from 19th March 2020 to 31st December 2022, treating the number of
30 hospital admissions in each region as an ordinal variable. We further developed the
31 XGBoost model used previously to forecast influenza to enable it to exploit the ordering
32 information in ordinal hospital admission levels. We incorporated different types of data as
33 predictors: epidemiological data including weekly region COVID-19 cases and hospital
34 admissions, weather conditions and mobility data for multiple categories of locations (e.g.,
35 parks, workplaces, etc). The impact of different discretisation methods and the number of
36 ordinal levels was also considered.

37 *Results*

38 We find that the inclusion of weather data consistently increases the accuracy of our
39 forecasts compared with models that rely only on the intrinsic epidemiological data, but only
40 by a small amount. Mobility data brings about a more substantial increase in our forecasts.
41 When both weather and mobility data are used in addition to the epidemiological data, the
42 results are very similar to the model with only epidemiological data and mobility data.

43 *Conclusion*

44 Accurate ordinal forecasts of COVID-19 hospitalisations can be obtained using XGBoost and
45 mobility data. While uniform ordinal levels show higher apparent accuracy, we recommend
46 N-tile ordinal levels which contain far richer information.

47 Author Summary

48 At the regional level, we address the pressing need for precise short-term forecasts of
49 respiratory infections, particularly COVID-19. We focus on the specific context of England
50 and cover the period from January 1 to December 31, 2022. We introduced an enhanced
51 XGBoost model that leverages the ordinal nature of hospital admission data, utilising a
52 combination of predictors, including epidemiological data, weather conditions, and mobility
53 data across various location categories. Our findings indicate that the inclusion of weather
54 data marginally improves forecasting accuracy, while mobility data yields more significant
55 enhancements. This research contributes valuable insights for public health agencies and
56 healthcare system managers in their ongoing efforts to manage and respond to the
57 complexities of the COVID-19 pandemic.

58 Introduction

59 The COVID-19 pandemic placed a considerable strain on hospitals at varying times and in
60 different locations between January 2020 and late 2021. By 31st December 2022, the World
61 Health Organization (WHO) has reported more than 600 million confirmed cases, including
62 6.6 million deaths [1]. Given the significant variation in disease incidence across both space
63 and time, even within the same country, local public health authorities often faced challenges
64 in obtaining adequate insights to effectively prioritise health services. This deficiency led to
65 even greater disruption in healthcare delivery than would have been otherwise anticipated.
66 Having advanced and accurate knowledge of higher disease incidence allowed for the
67 postponement of elective care, whereas insight into lower disease incidence facilitated a
68 more expedited refocusing on the backlog of postponed elective procedures. Heightened
69 levels of uncertainty were especially pronounced during the emergence of new COVID-19
70 variants, which were associated with increased transmission rates and, at times, greater
71 severity.

72 Specifically, in England and Wales, there were repeated rapid surges in SARS-CoV-2
73 infections, resulting in high demands for hospitalisations and medical resources for COVID-
74 19 patients. While vaccination efforts have significantly reduced the need for additional
75 interventions to prevent overwhelming hospitals, even as of December 2022, the persistently
76 high rates of infections and mortality have placed substantial pressure on the resources of
77 the National Health Service (NHS). Consequently, the need for frequently updated short-
78 term forecasting at the local level is evident, as it has the potential to markedly enhance the
79 efficiency with which limited healthcare capacity is employed [2].

80 Non-epidemiological time-varying factors may have collectively influenced the transmission
81 dynamics of SARS-CoV-2 [3,4]. Numerous studies have detailed the association between
82 COVID-19 cases and climate or meteorological conditions [5,6]. Multiple investigations
83 conducted in France have confirmed that the integration of weather factors into models can

84 enhance the model's capability to reproduce observed patterns, encompassing the
85 progression of hospital admissions [7,8].

86 Changes in human social behaviours swiftly impact the trajectory of an epidemic and the
87 influence of severe disease [9,10]. Comprehensive mobility data can be harnessed to
88 illustrate shifts in customary commuting behaviours, patterns of social interaction, and inter-
89 regional transits. These changes in metrics have shown correlations with infection rates and
90 mortality [11]. In this work, we endeavour to expand upon these findings by incorporating
91 weather conditions and mobility patterns into a model designed to predict COVID-19
92 admissions at the regional level.

93 Our previous work involved the development of a machine learning short-term forecasting
94 technique which demonstrated success through retrospective evaluations in predicting the
95 incidence of influenza-like illness (ILI) as an ordinal variable [12]. The method exhibited
96 satisfactory performance in these retrospective assessments. In this study, we expand upon
97 our previous method by integrating local weather conditions and mobility patterns to forecast
98 short-term, weekly COVID-19 admissions for seven NHS regions of England. As such, we
99 conduct a two-step evaluation of this novel method: 1) We examine whether the inclusion of
100 weather and mobility data enhances the accuracy of 1-to-4-week forecast individually and
101 collectively drawing from previous admission patterns; 2) We explore whether the machine
102 learning models can consistently achieve high accuracy across various levels of application.

103 **Methods**

104 *Data*

105 Our dataset amalgamates information encompassing epidemiological aspects of COVID-19
106 (hospital admissions, cases and deaths), human mobility patterns and weather data. All data
107 were sourced from publicly available outlets.

108 Epidemiological data were publicly available on the GOV.UK Coronavirus (COVID-19) in the
109 dashboard [13]. This source provided daily hospitalisation data for NHS regions in England,
110 capturing instances of positive COVID-19 tests within 14 days prior to hospitalisation, along
111 with post-admission positive cases. However, for NHS regions, daily cases and death
112 statistics were unavailable. Instead, we extracted case and death data for Lower Tier Local
113 Authorities (LTLAs) and subsequently matched the data of 315 LTLAs in England with their
114 respective NHS regions. This facilitated the aggregation of NHS region-specific- case and
115 death data. Daily death data recorded individuals who died within 28 days of being
116 confirmed COVID-19 cases, with the date reflecting the date of death instead of the date of
117 reporting. Hospital admission data became available on 19th March 2020 which postdates
118 the availability of case and death data. To ensure temporal consistency, the analysis
119 encompassed epidemiological data spanning from 19th March 2020 to 31st December 2022.

120 Daily hospitalisation, cases and deaths were aggregated by ISO week. Subsequently, the
121 weekly numbers were adjusted relative to the regional population, scaled per 100000
122 people, thereby generating per capita hospitalisation, cases and death statistics. The
123 regional population was deduced from population estimates at the LTLA levels by the Office
124 for National Statistics (ONS) [14]. Per capita cases and deaths remained as continuous
125 variables while per capita hospitalisation was converted into an ordinal variable using distinct
126 methodologies described below.

127 Per capita hospitalisation was converted into an ordinal variable with numerical levels
128 through two techniques: 1) N-tile, and 2) n-uniform interval, where $n = 3, 5,$ and 10. The N-
129 tile method constitutes an unsupervised discretisation method that segments the value range
130 into a specified number of bins (i.e., 3, 5 and 10 in this context), aiming to maintain nearly
131 uniform instances within each bin This effectively translates numeric target values into
132 ordinal quantities by ensuring equivalent-frequency binning. On the other hand, the n-
133 uniform interval strategy divides the range of values into equidistant bins, each containing
134 varying observation quantities. For both methodologies, the higher the value of the level, the
135 higher the number of hospital admissions, with level 1 representing minimal hospitalisation
136 and level n indicating the highest level of hospitalisation.

137 We collected human mobility data from Google, which provides aggregated anonymised
138 information sourced from its online platform [15]. This data provides insights into the
139 percentage changes in mobility across 7 different location categories, serving as a measure
140 of movement trends in response to the pandemic-related lockdowns. The reference point for
141 these trends is the baseline day, defined as the median value from 3rd January to 6th
142 February 2020. Each location category has its own specific baseline day. Google stopped
143 reporting new data on 15th October 2022.

144 While Google provides mobility data at the sub-regional levels for England, denoted by
145 *sub_region_1* and *sub_region_2* columns in the raw data, it is not readily compatible with
146 NHS regions. To address this, we used a combination of *sub_region_1* and *sub_region_2*
147 columns to map LTLA using a lookup table available on the GitHub repository
148 “*datasciencecampus / google-mobility-reports-data*” [16]. By calculating the mean daily
149 mobility values at the LTLA level and associating them with different NHS regions, we were
150 able to derive the daily mobility data for NHS regions. Finally, we obtained weekly mobility
151 data at the NHS-regional level by averaging the daily mobility by ISO weeks.

152 Our analysis also included weekly weather data, specifically air temperature at 2 meters (m)
153 and total precipitation, obtained from the fifth-generation reanalysis (ERA5) by the European
154 Centre for Medium-Range Weather Forecasts (ECMWF) [17]. To acquire data at the NHS-
155 regional level, we identified the nearest grid point to the centre of each of the 315 LTLAs and
156 calculated weekly temperature and total precipitation averages for the respective NHS
157 regions. Data types and predictors were summarised in Table 1.

158 **Table 1. Detailed descriptions of predictors.**

159

Data	Predictor	Description
Epidemiological data	Hospitalisation	COVID-19 Patients admitted to hospital; Ordinal variable.
	Cases	New cases by specimen date
	Deaths	New deaths with COVID-19 on the death certificate by date registered
	Region	NHS regions.
Weather data	Temperature	Air temperature at 2 meters (°C)
	Precipitation	Total precipitation (mm)
Mobility data	Grocery and pharmacy	Mobility trends for places such as grocery markets, food warehouses, farmers markets, speciality food shops, drug stores, pharmacies, etc.
	Parks	Mobility trends for places such as local parks, national parks, public beaches, marinas, dog parks, plazas, public gardens, etc.
	Transit stations	Mobility trends for places such as public transport hubs such as subway, bus, and train stations, etc.
	Retail and recreation	Mobility trends for places such as restaurants, cafes, shopping centres, theme parks, museums, libraries, movie theatres, etc.
	Residential	Mobility trends for residential places.
	Workplaces	Mobility trends for places of work.

160
161 *Primary forecast Model*

162 XGBoost is a standard classification algorithm for nominal classes, the ordinal information in
163 the class attributes may be discarded partly when applied to ordinal prediction problems,
164 while information can potentially enhance the predictability of the classifier. Therefore, we
165 used a simple method developed by [18] to enable the underlying learning algorithm,
166 standard XGBoost, in this work, to take advantage of the ordering information contained in
167 the hospital admission levels.

168 To utilise the ordered class values, the essential thought of this method is to transform a k -
169 class ordinal problem into a $k-1$ binary classification problem. This is achieved by converting
170 an ordinal attribute, denoted as A^* , with ordinal values V_1, V_2, V_3 , and so on up to V_k , into $k -$
171 1 binary attributes. Specifically, for each of the first $k-1$ values of the original attribute, a
172 binary attribute is created. Each of these binary attributes represents the test $A^* > V_i$, where i
173 refers to the corresponding value of the original attribute. By adopting this method, we can
174 effectively convert an ordinal regression problem into a binary classification problem, thereby
175 enabling the application of various binary classification algorithms to the original ordinal
176 problem.

177 The training process commences by generating novel datasets from the primary dataset,
178 where a distinct dataset is generated for each of the $k - 1$ newly formed binary class
179 attributes. We take $k = 5$ as an example here for illustration, i.e., hospital admissions are
180 divided into five levels, where the hospitalisation increases as the value of levels increases.
181 We then can convert it into 4 binary classification problems from the original dataset such
182 that

183 the binary target is i if levels $> i$, so the classifier will predict $Pr (Level > i)$ where $i = 1, 2, 3$
184 and 4

185 Subsequently, the XGBoost algorithm is applied to generate a model for each of the newly
186 created binary datasets separately. In order to predict the class value of an unseen instance,
187 it is necessary to estimate the probabilities of the k original ordinal classes, utilising the ($k -$
188 1) models developed in the previous step. The estimation of probabilities for the first and last
189 ordinal class values is determined by a single classifier. The probability of the first ordinal
190 value ($Level = 1$) is computed as $1 - Pr (Level > 1)$. In the same manner, the probability of
191 the last ordinal value ($Level = 5$) is determined by calculating the probability of $Pr (Level > 4)$.
192 For class values that fall within the range between 1 and 5, the probability is given by a pair

193 of classifiers. For example, the probability of $Pr(\text{Level} = 2)$ is given by $Pr(\text{Level} > 1) - Pr$
194 $(\text{Level} > 2)$.

195 Generally, for any ordinal hospital admission level values V_i the probability can be estimated
196 as:

$$197 \quad Pr(V_1) = 1 - Pr(\text{Level} > V_1)$$

$$198 \quad Pr(V_i) = Pr(\text{Level} > V_{i-1}) - Pr(\text{Level} > V_i), \quad 1 < i < k$$

$$199 \quad Pr(V_k) = 1 - Pr(\text{Level} > V_{k-1})$$

200 During the prediction phase, the $(k - 1)$ classifiers are involved in calculating the probability
201 of each of the k ordinal class values for an unknown instance by employing the
202 aforementioned approach. The class value with the highest probability is assigned to the
203 instance.

204 We applied the method described above to the standard XGBoost algorithm to construct a
205 new model that uses ordering information, referred to as the XGBoost ordered model in the
206 later section. The XGBoost ordered model is our primary forecast model and its performance
207 is evaluated in comparison with other baseline models. In addition, the standard XGBoost,
208 which treats each class attribute as a set of unordered values, was performed and compared
209 its performance to the ordered XGBoost model. For the purpose of distinction, in subsequent
210 sections, we refer to the standard XGBoost model as the XGBoost category model.

211

212 *Comparison null model*

213 Ordered logistic regression (OLR) was employed as a baseline model to serve as a
214 benchmark for evaluating the main model we explained above. The OLR model is an
215 extension of logistic regression, which assumes proportional odds where the effect of the
216 predictors is constant across all levels of the outcome variable [19]. It provides a simple but

217 useful starting point for exploring the relationship between the predictors and the ordinal
218 outcome. The predictors used in this model were limited to epidemiological predictors only
219 (prior one- and two-week hospitalisation levels and prior one-week cases and deaths).

220 In addition to the OLR model, the null model in which the prediction of the target week is the
221 same as the most recent available observation week, was used as a baseline model as well.

222

223 *Combinations of predictors*

224 Hospital admission level is the ordinal outcome for each model. Three types of data were
225 incorporated as predictors in the models: 1) epidemiological data, including ordinal
226 hospitalisation levels, COVID-19 cases and deaths; 2) weather data, including temperature
227 and total precipitation; 3) community mobility trends data in different types of locations. We
228 only applied epidemiological data to the baseline models to provide baseline accuracy for
229 model evaluation. For the XGBoost ordered and category models, we adapted four different
230 combinations of predictors: 1) epidemiological data only; 2) epidemiological and weather
231 data; 3) epidemiological and mobility data and 4) epidemiological, weather and mobility data.
232 Detailed descriptions of data and predictors used for each model are summarised in Table 2.

233

234

235

236

237

238

239

240

241

242

243

244

245 **Table 2. Summary of predictors incorporated by each model.**

Model	Predictor
Baseline model 1 - Null model	Epidemiological data
Baseline model 2 - OLR	Epidemiological data
XGBoost category model	Epidemiological data Epidemiological data + Weather conditions Epidemiological data + Mobility data Epidemiological data + Weather conditon + Mobility data
XGBoost ordered model	Epidemiological data Epidemiological data + Weather conditions Epidemiological data + Mobility data Epidemiological data + Weather conditon + Mobility data

246

247 *Forecasting*

248 The COVID-19 hospitalisation data can be characterised as a non-stationary time series,
 249 with a notable autocorrelation. Rather than employing a random data split for training and
 250 test sets, we made a deliberate choice. We designated the period from 9th March 2020 to
 251 31st December 2021 as the training set, and the timeframe spanning from 1st January to
 252 31st December 2022 as the test set. We also implemented the extending window approach,
 253 as previously detailed in our work [12] to facilitate multiple-step-ahead forecasts. In brief, we
 254 augmented the fitted period (i.e., the training set) with one new observation during each
 255 forecasting update. This methodology in defining training and test sets was consistently
 256 applied across all the models used in this work.

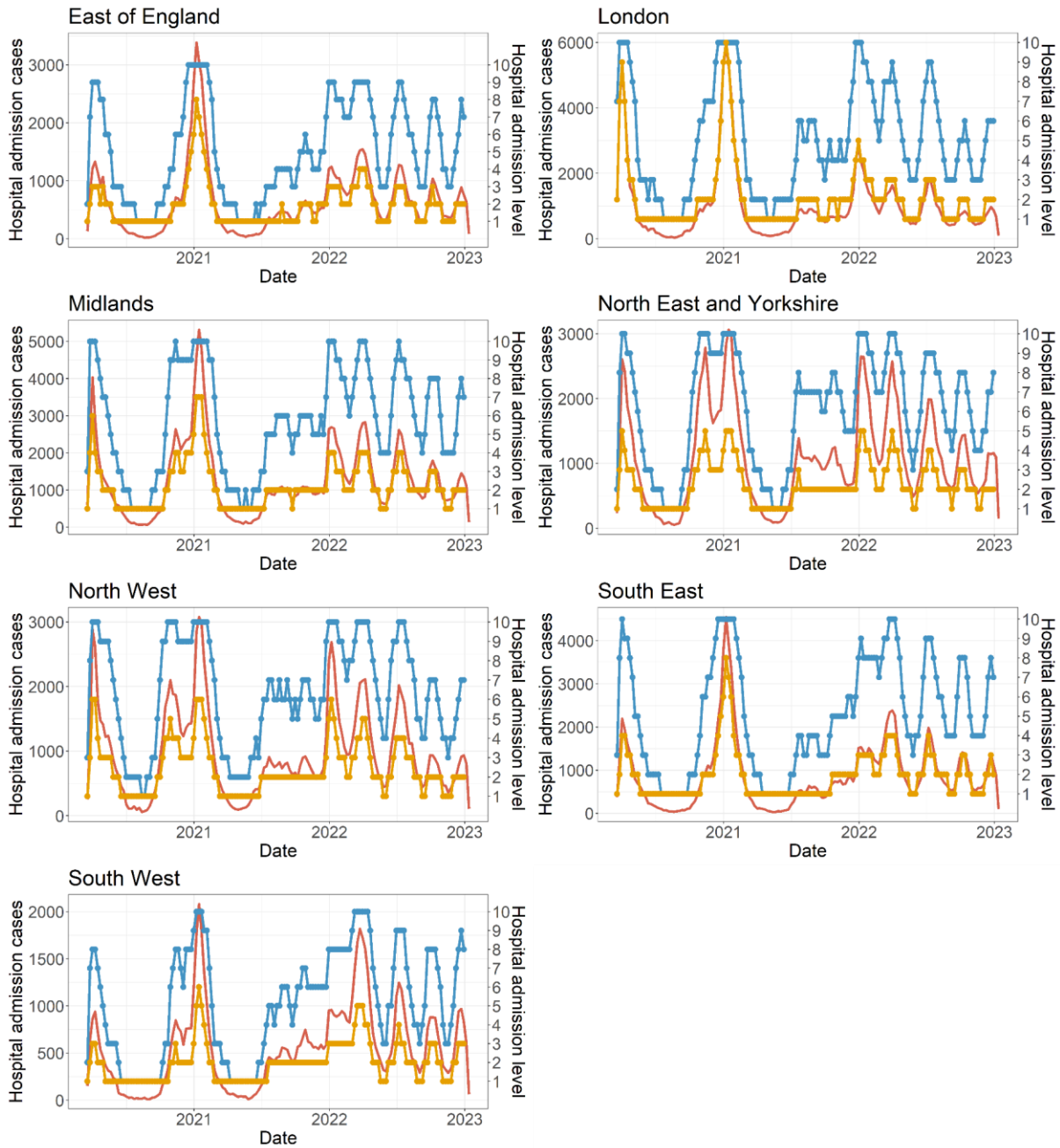
257 In terms of the hyperparameters for both the standard XGBoost model and XGboost ordered
 258 model, we maintained the same values that have been fine-tuned in our earlier work (Table
 259 S1) [12]. The analysis was conducted in R version 4.1.3.

260 *Evaluation metrics*

261 We assessed the models based on two key metrics: macro-averaged mean absolute error
262 (mMAE) and accuracy. Macro-averaged mean absolute error (mMAE) refers to the average
263 of the mean absolute error (MAE) calculated for each class. More detailed explanations can
264 be found in [12]. Accuracy is defined as the proportion of the number of weeks in which
265 hospitalisation levels were correctly predicted to the total number of weeks within the test
266 period.

267 Results

268 Critical analysis of the COVID-19 pandemic in England reveals several significant trends
269 related to the timing and magnitude of peaks in healthcare demand. These patterns are
270 evident when examining both the raw hospitalisation data and an N-tile ordinal
271 representation (Figure 1). Notably, during the dominance of the Alpha variant, hospitalisation
272 reached its peak across all the NHS regions in January 2021. However, with the
273 implementation of the third national lockdown and the rollout of vaccination programs and
274 public health initiatives, hospitalisation rates gradually declined throughout the spring and
275 summer months. The emergence of the Delta variants in mid-2021 marked a concerning
276 shift as hospitalisations once again began to surge during the autumn and early winter of
277 that year. Subsequently, the arrival of the Omicron variant in late 2021 ushered in yet
278 another wave of increased hospitalisations, which persisted into the early months of 2022.
279 Following this, the hospitalisation levels exhibited a fluctuating downtrend trajectory.



280 Hospitalisation — Hospital admission cases — Hospital admission level (n-tile) — Hospital admission level (uniform)
 281 **Figure 1. Epidemic curve of weekly hospitalisation by NHS regions in England from 19**
 282 **March 2020 to 31 December 2022.** The left y-axis represents the weekly count of new
 283 hospital admissions (red line), while the right y-axis depicts the weekly hospitalisation level
 284 determined using the N-tile method (blue line) and the uniform method (yellow line), with a
 285 total of 10 district levels.

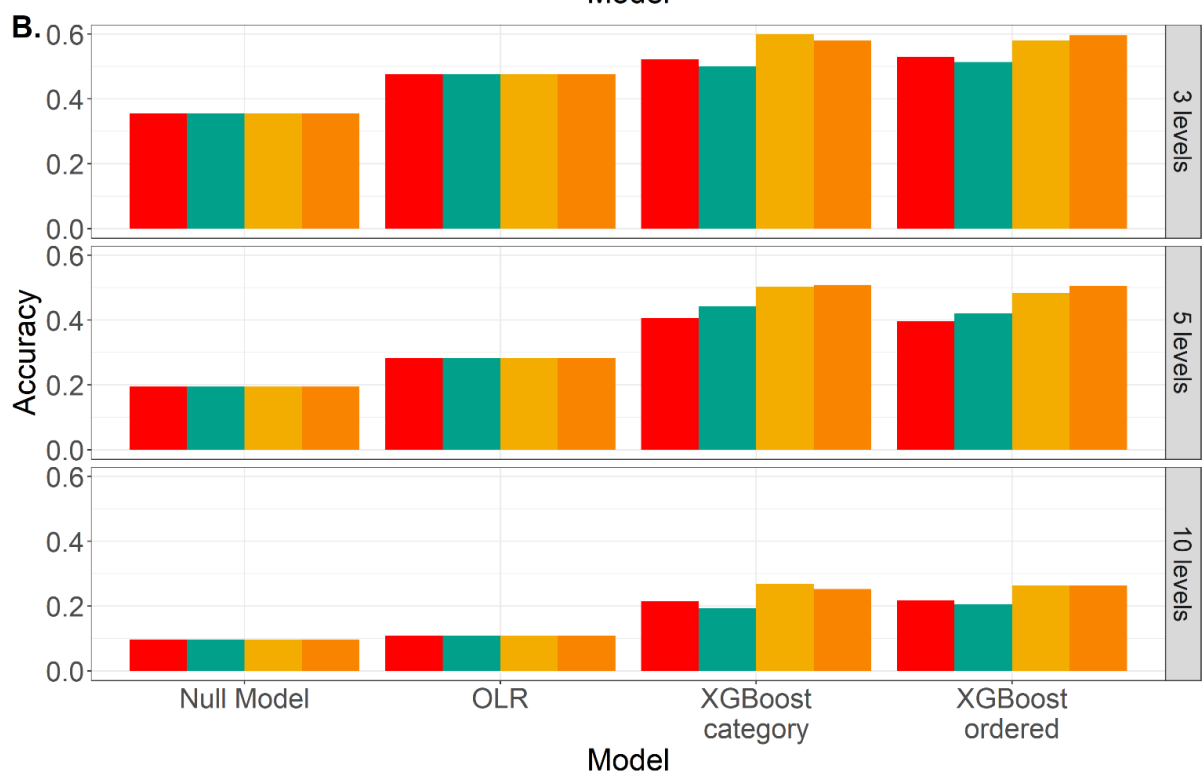
286
287 Examining regional COVID-19 hospitalisation data from England provides a valuable
288 opportunity to demonstrate the distinctions between the N-tile ordinal version of this data.
289 Notably, the frequency distribution does not effectively differentiate between the ordinal
290 levels as defined by the uniform method (S1 Figure). For instance, when using three levels,
291 an overwhelming 90.02% of observations fall into level 1. With 5 levels, 94.81% of data
292 points cluster within levels 1 and 2; while with 10 levels, a substantial 88% of the
293 observations falls between 1 and 3. Consequently, the ordinal levels derived from the
294 uniform approach appear to display a smoother and less fluctuating trend when compared to
295 the actual numerical trend (Figure 1, S2 Figure). Therefore, we have opted to use the N-tile
296 levels as our primary outcome and focus on assessing the predictive performance of models
297 using the ordinal outcome established by the N-tile method. We will revisit the potential
298 impact of this choice in a subsequent sensitivity analysis.

299 Our initial evaluation of model performance exclusively considered epidemiological data,
300 which may be the only option for many populations during future similar periods.

301 Surprisingly, we consistently achieved more accurate forecasts by the XGboost ordered
302 model when compared to baseline models for 1- to 4-week ahead predictions even without
303 incorporating additional potential features such as weather and mobility in the model (S3
304 Figure).

305 Subsequently, we introduced weather and mobility data as predictors into both the XGBoost
306 ordered and category models evaluating model performance by macro-averaged Mean
307 Absolute Error (mMAE). The mMAE was computed as the average value across seven NHS
308 regions. Incorporating weather data alongside epidemiological data indeed improved the
309 performance of our forecasting models when compared to baseline models (Figure 2).

310 However, when comparing XGBoost models featuring both weather and epidemiological
311 data with those utilising only epidemiological data, there was no improvement in accuracy
312 (S4 Figure).



Data █ Epi* features █ Epi*+Weather features █ Epi*+Mobility features █ Epi*+Mobility+Weather features

314 **Figure 2. Accuracy metrics comparison of 4-week ahead forecasts between models**
315 **trained with different combinations of predictors. A.** Average macro-averaged Mean
316 Absolute Error (mMAE) over all seven NHS regions. **B.** Average accuracy over all seven
317 NHS regions.

318 *Epidemiological

319

320 In contrast, our findings suggest that the mobility data significantly enhances forecast
321 accuracy compared to relying solely on epidemiological data alone (Figure 2). Notably, the
322 XGBoost model that exclusively incorporates epidemiological data consistently performed
323 notably worse than those integrating mobility data (S5 Figure). This underscores the
324 importance of mobility data as a crucial factor in COVID-19 hospitalisation forecasting
325 models.

326 Finally, we incorporated both mobility and weather data into the models. Figure 3 illustrates
327 the average mMAE for each of the four combinations of predictors in the XGBoost models
328 across various prediction horizons (1- to 4-week ahead). Within each prediction horizon,
329 mMAE increases as the prediction horizon increases, highlighting the increased challenge of
330 making predictions further ahead in time. Nevertheless, across all prediction horizons,
331 models that incorporate mobility data consistently demonstrate superior performance.
332 Particularly noteworthy is the reduction in mMAE for 3- and 4-week ahead prediction when
333 both weather and mobility are used as predictors.

334 We also investigated the relative merits of different numbers of ordinal levels and Table 2
335 summarises the results for the 3-, 5-, and 10-bin levels based on the N-tile bins. It becomes
336 evident that the XGBoost ordered model consistently outperforms the baseline models in
337 terms of accuracy for both 3 and 5 bins defined by the N-tile method. However, it is
338 interesting to note that the XGBoost ordered model does not always exhibit a significantly
339 superior performance. For the 10-bin scenario, we observe more substantial differences in

340 accuracy (Table 3, Figure 3), in particular when comparing it to the XGBoost category model
341 under the N-tile method. In this context, the divergence in performance between the
342 XGBoost ordered model and the baseline models becomes more significant. Moreover, the
343 XGBoost surpasses the XGBoost category model across all four predictor combinations and
344 prediction horizons. This substantial improvement underscores the increasing relevance of
345 ordering information as the number of classes increases (Figure 4).

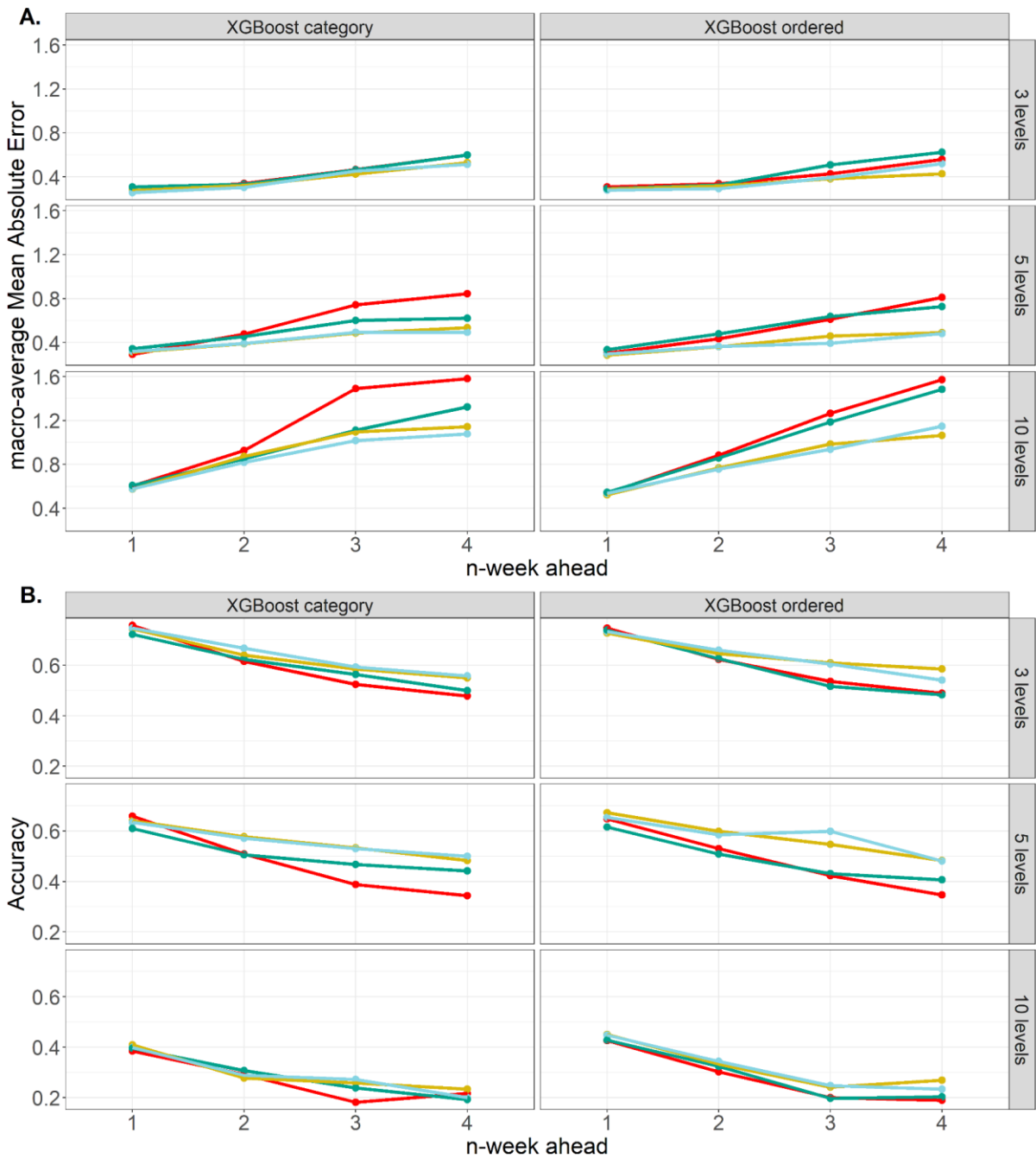
346

347 **Table 3. Predictive performance of models when the N-tile method is used to define the ordinal level of hospital admissions.**

n-week ahead		Bins = 3		Bins = 5		Bins = 10	
		mMA E	Accuracy (%)	mMA E	Accuracy (%)	mMA E	Accuracy (%)
1-week ahead	Null model	0.294	76.92%	0.290	66.48%	0.604	39.29%
	OLR	0.302	73.47%	0.317	60.88%	0.498	44.56%
	XGBoost category	0.298	72.80%	0.305	64.56%	0.605	37.91%
	XGBoost ordered	0.293	71.43%	0.279	67.03%	0.494	45.60%
2-week ahead	Null model	0.536	56.59%	0.540	43.41%	1.088	23.35%
	OLR	0.503	55.78%	0.424	47.28%	0.960	24.49%
	XGBoost category	0.315	65.38%	0.376	58.79%	0.811	31.87%
	XGBoost ordered	0.300	65.93%	0.340	61.26%	0.668	35.44%
3-week ahead	Null model	0.717	42.03%	0.793	28.57%	1.593	13.46%
	OLR	0.540	54.08%	0.624	38.78%	1.366	18.37%
	XGBoost category	0.349	61.81%	0.473	55.77%	0.971	29.40%
	XGBoost ordered	0.346	64.56%	0.388	60.44%	0.832	28.85%
4-week ahead	Null model	0.888	35.44%	1.011	19.51%	1.974	9.62%
	OLR	0.663	47.62%	0.891	28.23%	1.874	10.88%
	XGBoost category	0.483	57.97%	0.470	50.82%	1.024	25.27%
	XGBoost ordered	0.427	59.62%	0.475	50.55%	1.002	26.37%

348

349

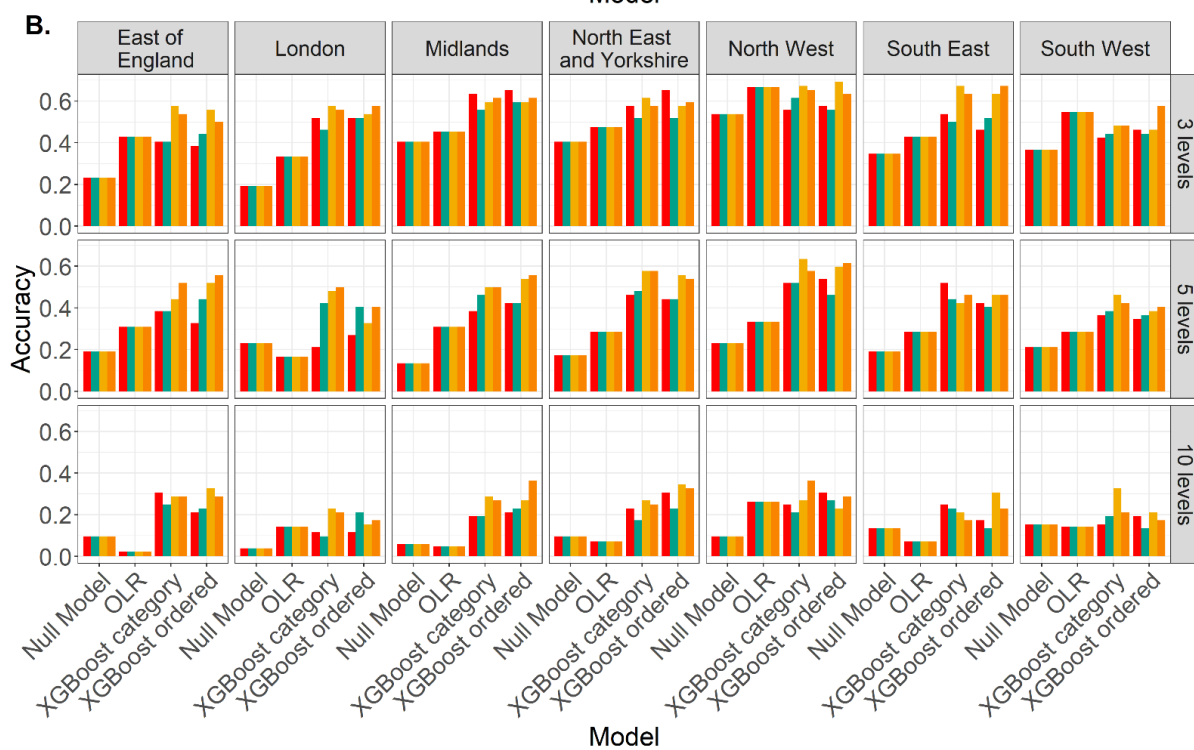
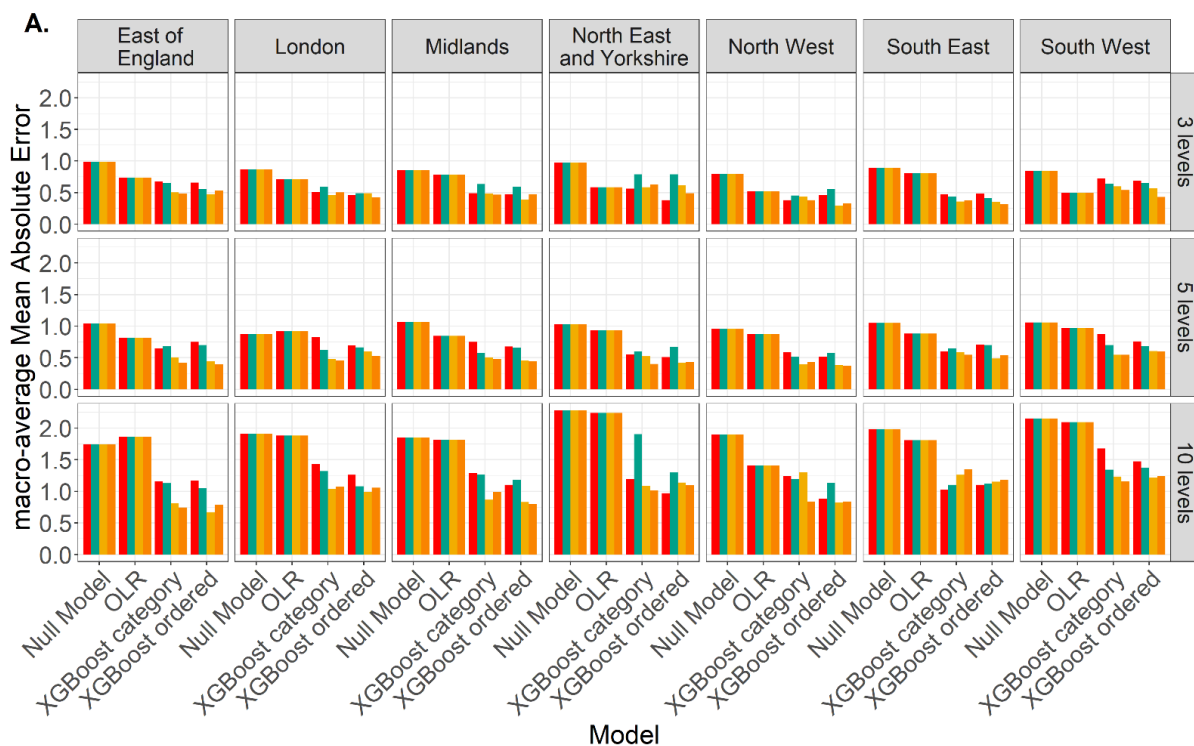


350

Data ● Epi* features ● Epi*+Weather features ● Epi*+Mobility features ● Epi*+Mobility+Weather features

351 **Figure 3. Evaluating XGBoost model performance with various feature sets, using**
352 **macro-averaged Mean Absolute Error (mMAE) and accuracy.** The overall mMAE was
353 computed by averaging across the seven NHS regions for each prediction horizon spanning
354 from 1- to 4-week ahead). **A.** mMAE of both the XGBoost category model and the XGBoost
355 ordered model trained with the following sets of features 1) epidemiological data (red line); 2)
356 epidemiological and weather data (green line); 3) epidemiological and mobility data (yellow
357 line); and 4) epidemiological, mobility and weather features (blue line). **B.** Accuracy results
358 for the XGBoost category model and the XGBoost ordered model, which was trained using
359 the same feature sets as in Panel A with 1) epidemiological data (red line); 2)
360 epidemiological and weather data (green line); 3) epidemiological and mobility data (yellow
361 line); and 4) epidemiological, mobility and weather features (blue line).

362 *Epidemiological



363

364 **Figure 4. Comparison of model performance by NHS regions for XGBoost models and**
365 **baseline models trained with different combinations of predictors when the prediction**
366 **horizon is 4 week-ahead for the test period 2022.** The levels are defined by the N-tile
367 method. **A.** mMAEs of forecasts for hospitalisation levels. **B.** Accuracy of forecasts for
368 hospitalisation levels.

369 *Epidemiological

370

371 To assess the significance of predictors, we used “the Gain”, a metric that quantifies the
372 relative contribution of each feature to the XGBoost ordered model. The five most influential
373 predictors are as follows: hospitalisation levels from previous weeks, the number of COVID-
374 19 cases, temperature, mobility changes in retail and recreation places, and the number of
375 COVID-19-associated deaths (Figure S6). These key predictors underscored the importance
376 of epidemiological data and how the inclusion of weather and mobility data further enhances
377 the model's accuracy. Conversely, total precipitation and other mobility trends exhibit lower
378 importance in the model.

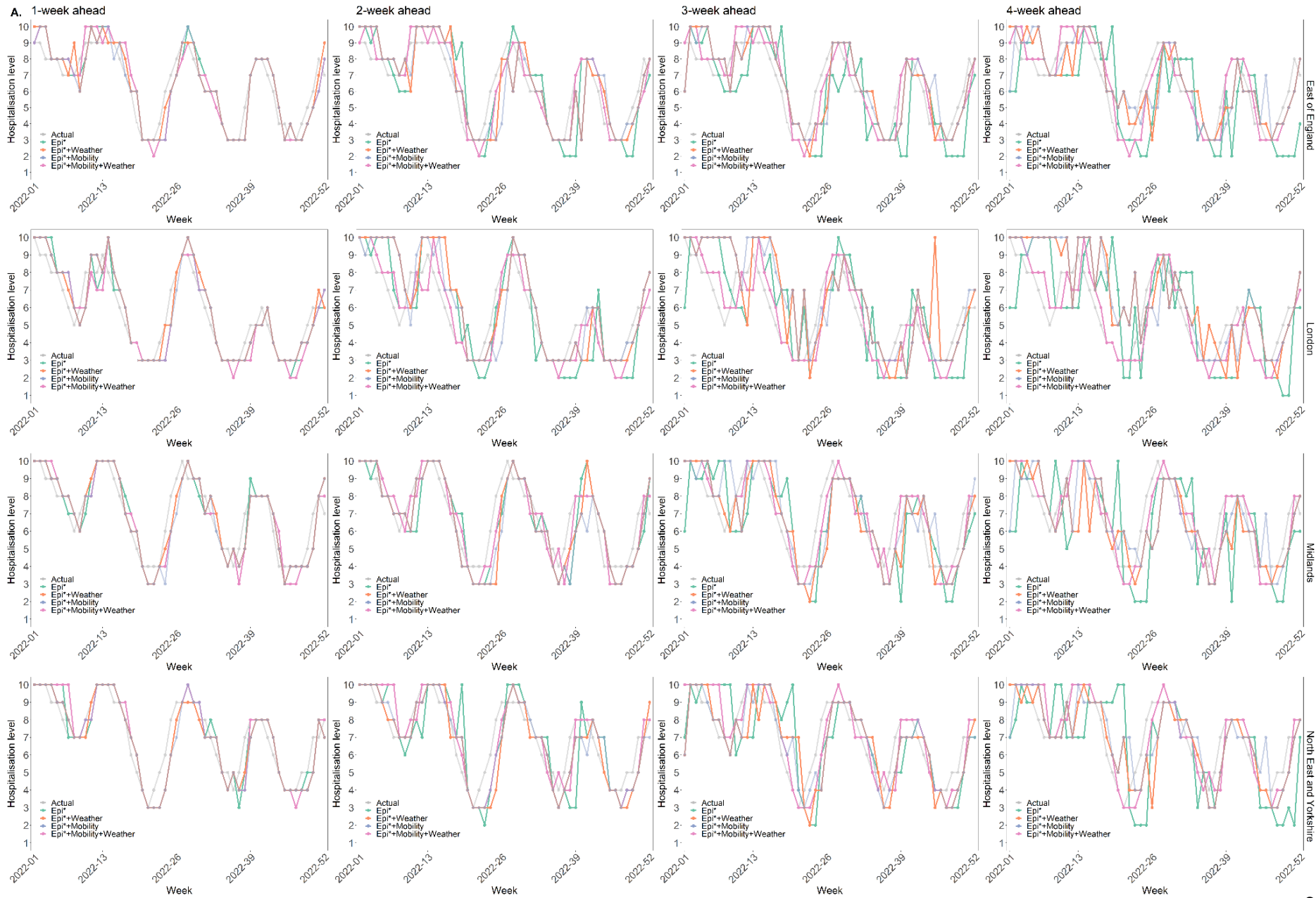
379 Our findings are corroborated when we compare results across individual regions (Figure 5).
380 Using the N-tile method to define hospitalisation levels, we predicted these levels 1- to 4-
381 week ahead throughout the entire test period. Notably, the prediction errors (mMAEs) are
382 consistently lower in models that feature mobility data and even lower when both mobility
383 and weather data are included, as compared to using only epidemiological or weather alone
384 for all regions. As the ordinal class value increases, the discrepancy in prediction errors
385 becomes more pronounced. For instance, in the East of England, when the class number is
386 set to 10, the mMAE of the 2-week ahead forecast only uses epidemiological data is about
387 double that of a 4-week ahead forecast incorporating both weather and mobility data. When
388 extending the prediction horizon to 4-week ahead, the difference in mMAE increases
389 threefold.

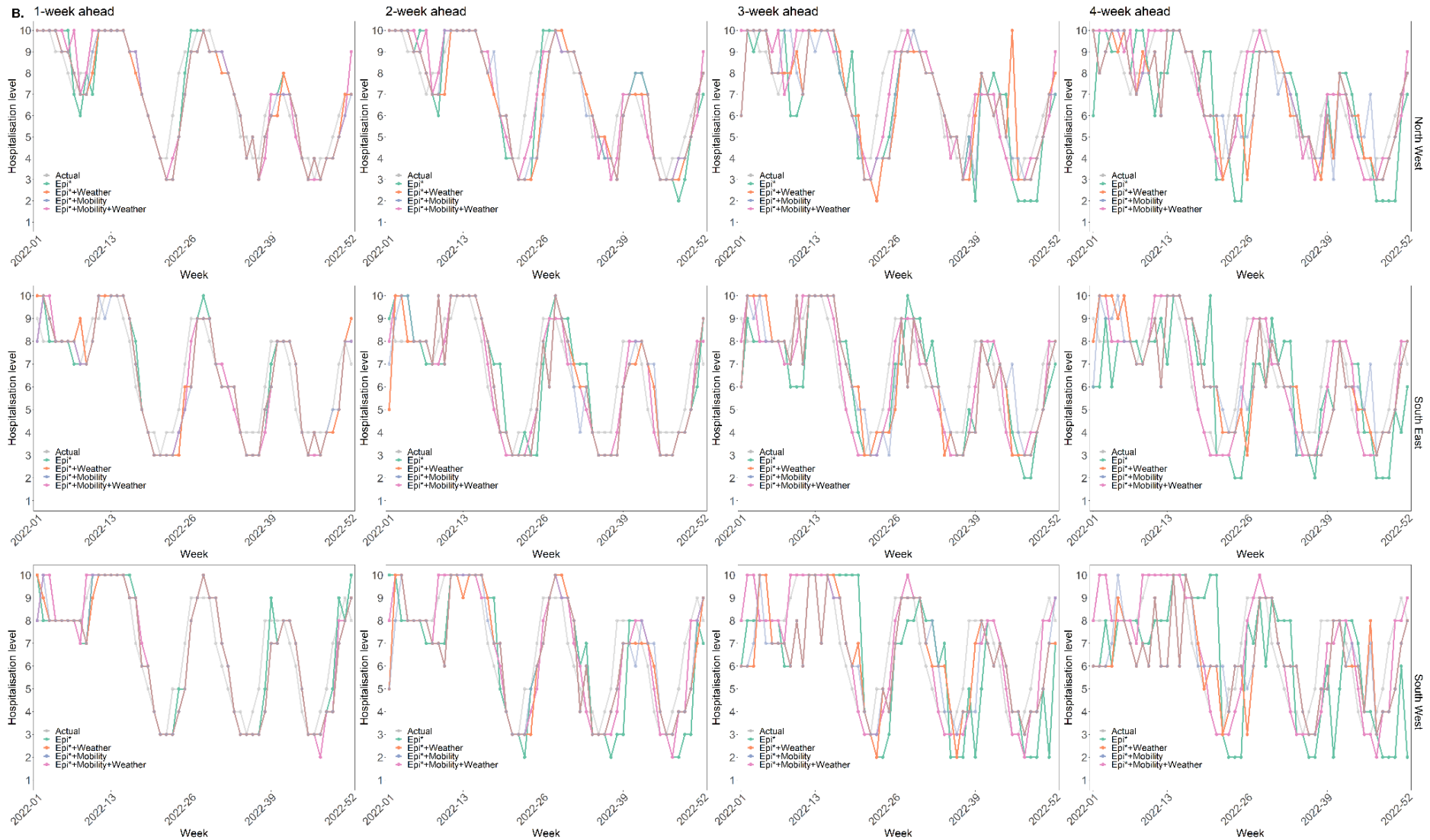
391 **Figure 5.** Comparison of NHS-region-specific performance for the XGBoost ordered model
392 trained with 1) epidemiological features (beige line); 2) epidemiological and weather features
393 (pink line); 3) epidemiological and mobility features (brown line); and 4) epidemiological,
394 weather and mobility features (yellow line). The prediction horizon is from 1 to 4 week-ahead
395 for the test period 2022. The number of total levels orders the rows from 3 (top) to 10
396 (bottom) levels, and levels are defined by the N-tile method. Each column represents one
397 NHS region. **A.** mMAEs of forecasts for hospitalisation levels. **B.** Accuracy of forecasts for
398 hospitalisation levels.

399 *Epidemiological

400

401 In Figure 6, we conducted a comparative analysis between the predicted values generated
402 by the XGBoost ordered models and the time series data representing actual hospitalisation
403 values. Across all NHS regions, all four predictor combinations effectively capture the overall
404 hospitalisation trends and successfully identify the peak admission levels for 1- and 2-week
405 forecasts. Particularly noteworthy is the superior accuracy of models incorporating mobility
406 data and models combining both mobility and weather data. However, when looking at 3-
407 and 4-week ahead forecasts, the model relying solely on epidemiological data exhibits
408 noticeable deviations from the actual levels, primarily evident in a lag in predicting peak
409 admissions. For these longer-term forecasts, the models integrating mobility data, and
410 especially those incorporating both mobility and weather data, do not entirely capture the
411 fluctuations observed at the beginning of 2020. Nonetheless, their predictions for up to 4-
412 weeks ahead remain the closest approximation to the actual observed peak, emphasizing
413 their predictive strength even in the face of more extended forecasting horizons.





416 **Figure 6. Comparison of actual and predicted hospitalisation levels by NHS regions.**

417 The predicted hospitalisation levels are predicted by the XGBoost ordered model with 10
418 levels defined by the N-tile method, and the time ranges from week 1 to week 52 in 2022.
419 Each row represents one NHS region. Columns are prediction horizons ordered from 1- (left)
420 to 4-week (right) ahead. **A.** East of England, London, Midlands and North East and
421 Yorkshire; **B.** North West, South East and South West.

422

423 Discussion

424 This study aims to enhance the accuracy of forecasting regional hospitalisation levels in
425 England, which are treated as ordinal outcomes, by integrating various data sources. We
426 evaluated the efficacy of different bin partitioning methods in leveraging the inherent ordering
427 information. Notably, the N-tile method outperforms the uniform method in this regard. Our
428 study covered seven NHS regions and assesses the performance of short-term forecasts in
429 three distinct scenarios: 1) forecasts solely reliant on epidemiological data, including
430 previous hospitalisation figures, case counts, and mortality statistics; 2) forecasts that
431 incorporate mobility data and weather conditions as supplementary predictors, considered
432 separately from epidemiological data; 3) forecasts that incorporate both mobility data and
433 weather conditions as additional predictors alongside epidemiological data.

434 Our findings reveal that the XGboost ordered model, based solely on epidemiological data,
435 achieves superior accuracy compared to baseline models. This outcome is particularly
436 beneficial for countries with limited access to diverse data sources beyond epidemiological
437 data. Furthermore, we provide evidence that the inclusion of aggregated mobility data
438 significantly enhances prediction accuracy, extending up to a 4-week horizon when
439 compared to models relying solely on epidemiological data. However, our analysis indicates
440 that the contribution of weather conditions to prediction accuracy is minimal.

441 A key insight from our study is the strong predictive power of mobility data in relation to
442 COVID-19 transmission compared to weather conditions. Our findings are consistent with
443 prior research that underscored the pivotal role of mobility as a primary predictor of COVID-
444 19 transmission dynamics [20–23]. Several other studies have also explored the association
445 between mobility and COVID-19 transmission but have arrived at varying conclusions. For
446 instance, a study conducted by [24] found mobility to be a significant predictor of COVID-19
447 cases in specific regions, while observing limited impact in others. Meanwhile, [25]
448 demonstrated a strong correlation between mobility and COVID-19 transmission across
449 diverse geographical areas. These disparities in findings may be attributed to differences in
450 study design, regional or geographical contexts, and specific modelling approaches
451 employed. Differences in data collection methods and time periods considered in each study
452 may also contribute to the observed discrepancies. In our analysis, we believe that the
453 extensive and diverse dataset we used, allowed us to discern mobility as the primary
454 predictor. Additionally, the incorporation of local factors and spatiotemporal variations in
455 mobility patterns might have contributed to our more accurate predictions.

456 Mobility data reflects the contact behaviour changes occurring within a population in
457 response to COVID-19, while weather factors may interact with these changes and
458 contribute to the spread of COVID-19, potentially leading to increased hospitalisation. For
459 example, during mild weather conditions, individuals tend to spend more time outdoors in
460 parks and engage in socialising activities involving close contact without adhering to safety
461 measures such as wearing masks and physical distancing.

462 Nonetheless, our study has its limitations. First, we assumed that aggregated mobility data
463 captures well the human social mixing patterns in the population. The robustness of our
464 model forecasts relies heavily on the accessibility and representativeness of this aggregate
465 mobility data. It is important to note that Google ceased updating their mobility data from 15
466 October 2022 onwards, which may limit the generalisability of our results in the future due to
467 the reduced availability of mobility datasets. Moreover, in resource-constrained settings with

468 limited smartphone usage, the aggregated mobility data may not fully characterise the
469 movement patterns of the entire population.

470 Furthermore, the lack of continuous and long-term availability of mobility or weather data in
471 certain resource-constrained regions or countries is another constraint. Consequently, the
472 generalisability of our findings may be impacted, as the reduced availability of mobility and
473 weather datasets could hinder the accurate assessment and prediction of the transmission
474 dynamics of COVID-19 in those areas. For these reasons, we also described here the
475 performance of the XGBoost model of ordinal data using only intrinsic variables in the time
476 series.

477 We were unable to obtain sufficiently accurate datasets to consider the incorporation of non-
478 pharmaceutical interventions (NPIs) and vaccination as additional features in our predictive
479 model at the regional level. Specifically, the absence of suitable weekly vaccination data by
480 NHS regions hindered our ability to assess the potential influence of vaccination coverage
481 rates on the accuracy of our predictions. Furthermore, we did not include factors such as the
482 effectiveness of NPIs and behavioural patterns, such as intentions of wearing face masks
483 and following social distancing, as predictors in our model. However, it is widely
484 acknowledged that vaccination and non-pharmaceutical interventions have played pivotal
485 roles in mitigating the spread of COVID-19 and reducing infection and hospitalisation rates in
486 various regions[26,27]. The rollout of vaccination campaigns and the implementation of
487 NPIs, including lockdowns, travel restrictions, and mask mandates, have demonstrated their
488 efficacy in curbing transmission and alleviating the strain on healthcare systems[28,29]. We
489 propose that the framework we have outlined here could be effectively employed when such
490 data become available, allowing for the assessment of the potential value of these variables
491 in predicting critical hospitalisation patterns.

492 Considering the significant impact of vaccination and NPIs on disease transmission
493 dynamics, we acknowledge the critical importance of integrating these factors in future

494 modelling efforts. The inclusion of vaccination coverage rates, NPI implementation timelines,
495 and compliance levels with behavioural interventions would enrich our predictive model and
496 enhance its accuracy in forecasting COVID-19 trends at the regional levels. These
497 enhancements could facilitate more precise and timely public health decision-making and
498 resource allocation during pandemic management. To advance this effort, it is imperative to
499 have access to available and reliable datasets encompassing vaccination coverage and NPI
500 implementation across NHS regions. Robust data collection and reporting mechanisms are
501 essential for researchers and policymakers to gain a comprehensive understanding of the
502 interplay between vaccination efforts, NPI adoption, and disease transmission
503 dynamics[30,31]. Collaborative initiatives among healthcare agencies, governmental bodies,
504 and research institutions are also important for establishing standardised data collection
505 protocols and enabling the timely sharing of accurate information.

506 In conclusion, our findings underscore the value of incorporating weather and mobility data
507 to explore the ordering information of ordinal hospitalisation levels, thereby enhancing the
508 precision of hospital admission level predictions over a 4-week ahead time horizon. This
509 extension provides policymakers with additional time to plan and allocate hospital resources
510 effectively.

511

512 Supporting information

513 **S1 Table. Hyperparameter values used by the XGBoost models.**

514 (XLSX)

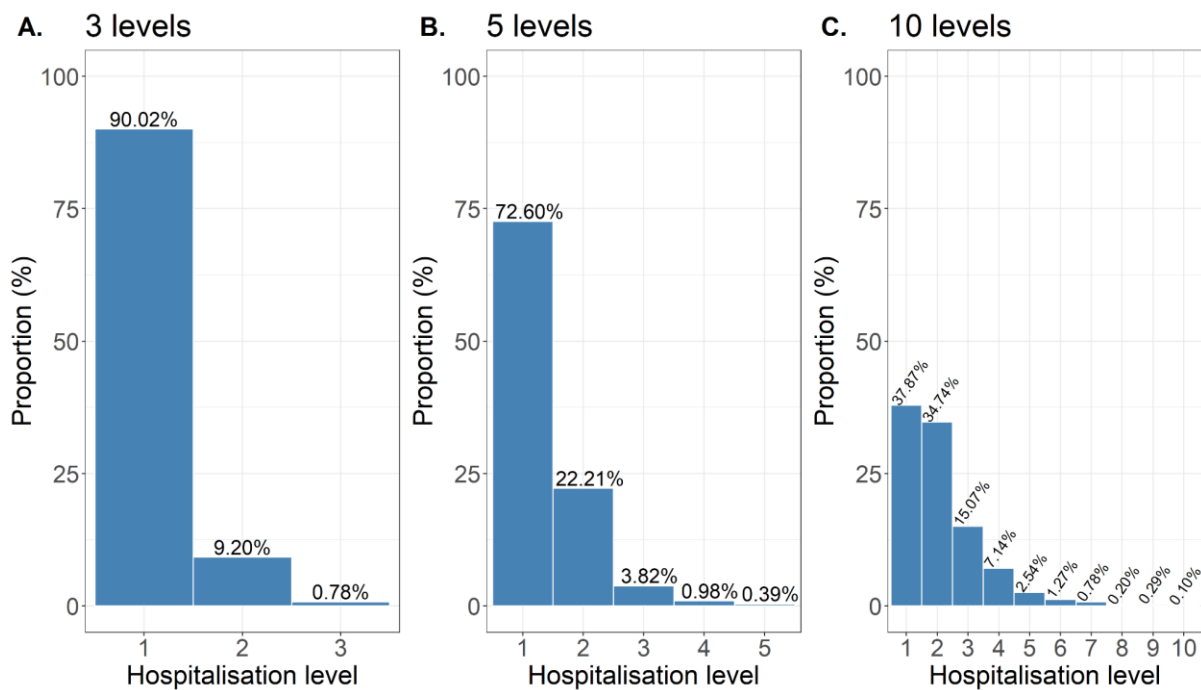
515

516 **S2 Table. Predictive performance of models when the ordinal level of hospital**

517 **admissions is defined by the uniform method.**

518 (XLSX)

519



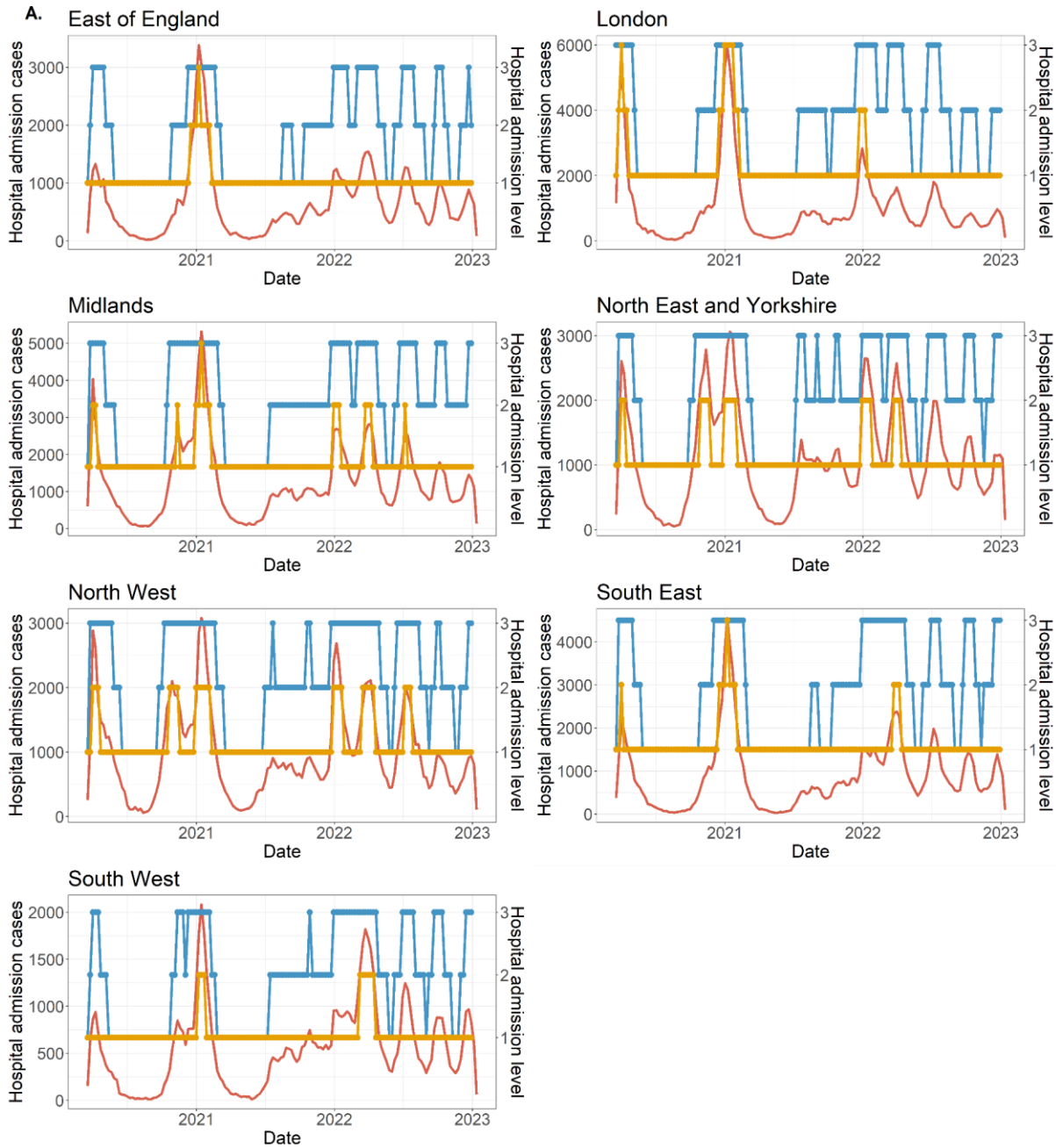
520

521 **S1 Figure. Distribution of ordinal levels for weekly hospitalisations for NHS regions**

522 **discretised by the uniform method. A.** The distribution of hospital admission that

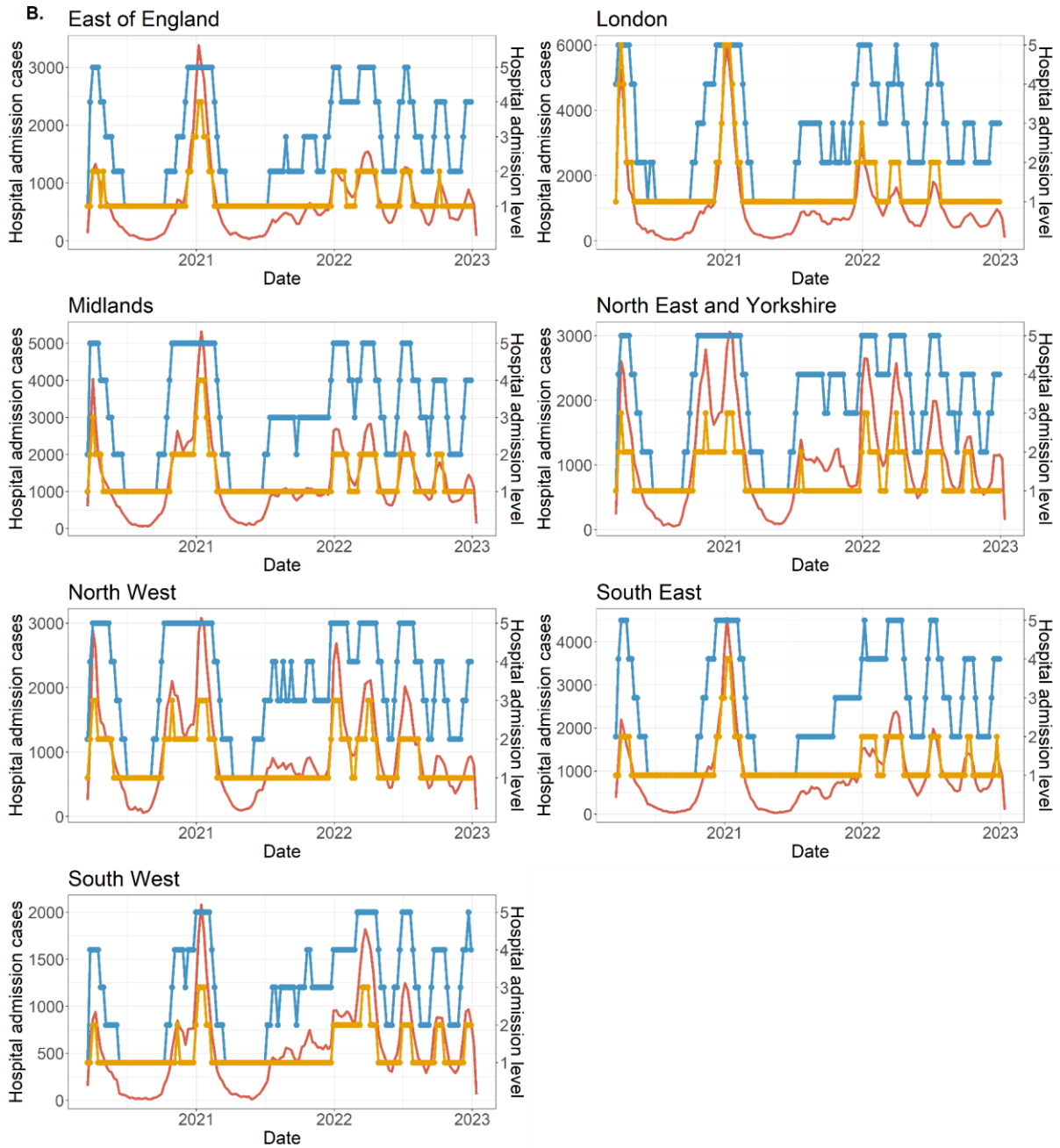
523 discretised into three levels. **B.** The distribution of hospital admission that discretised into

524 five levels. **C.** The distribution of hospital admission that discretised into ten levels.



525 Hospitalisation — Hospital admission cases — Hospital admission level (n-tile) — Hospital admission level (uniform)

526



527 Hospitalisation - Hospital admission cases - Hospital admission level (n-tile) - Hospital admission level (uniform)

528

529

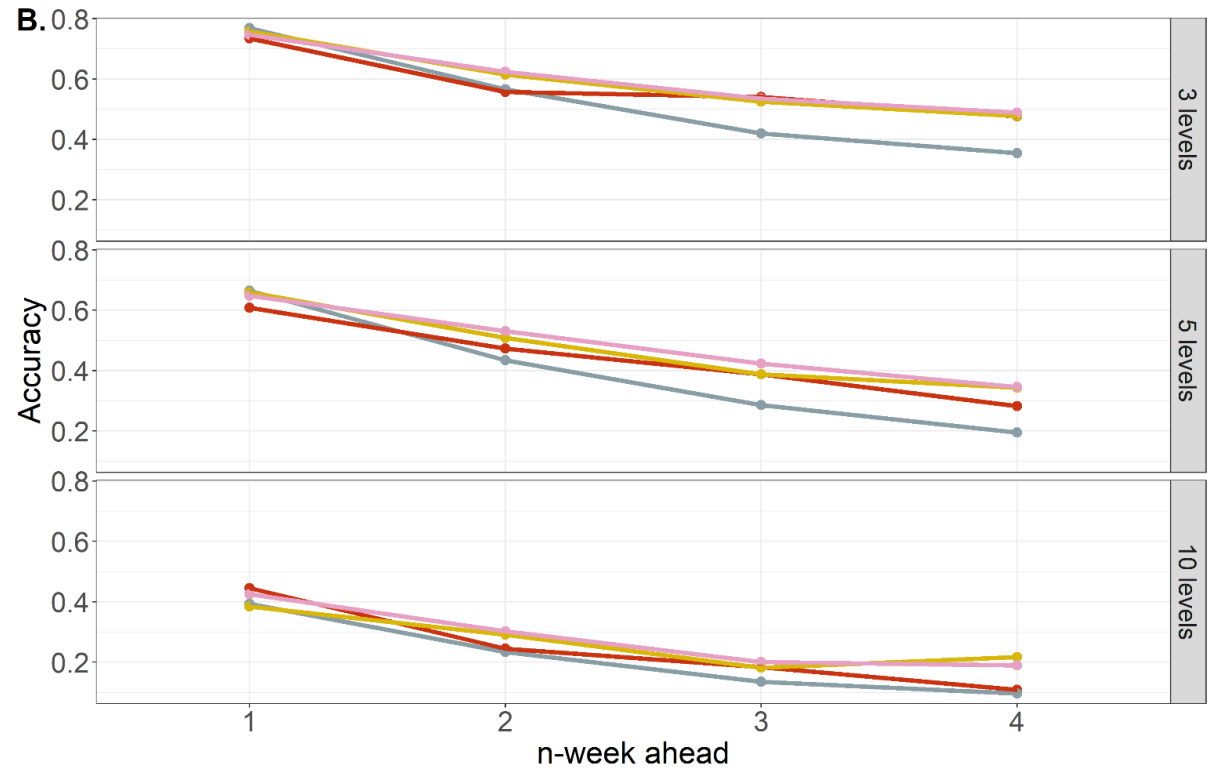
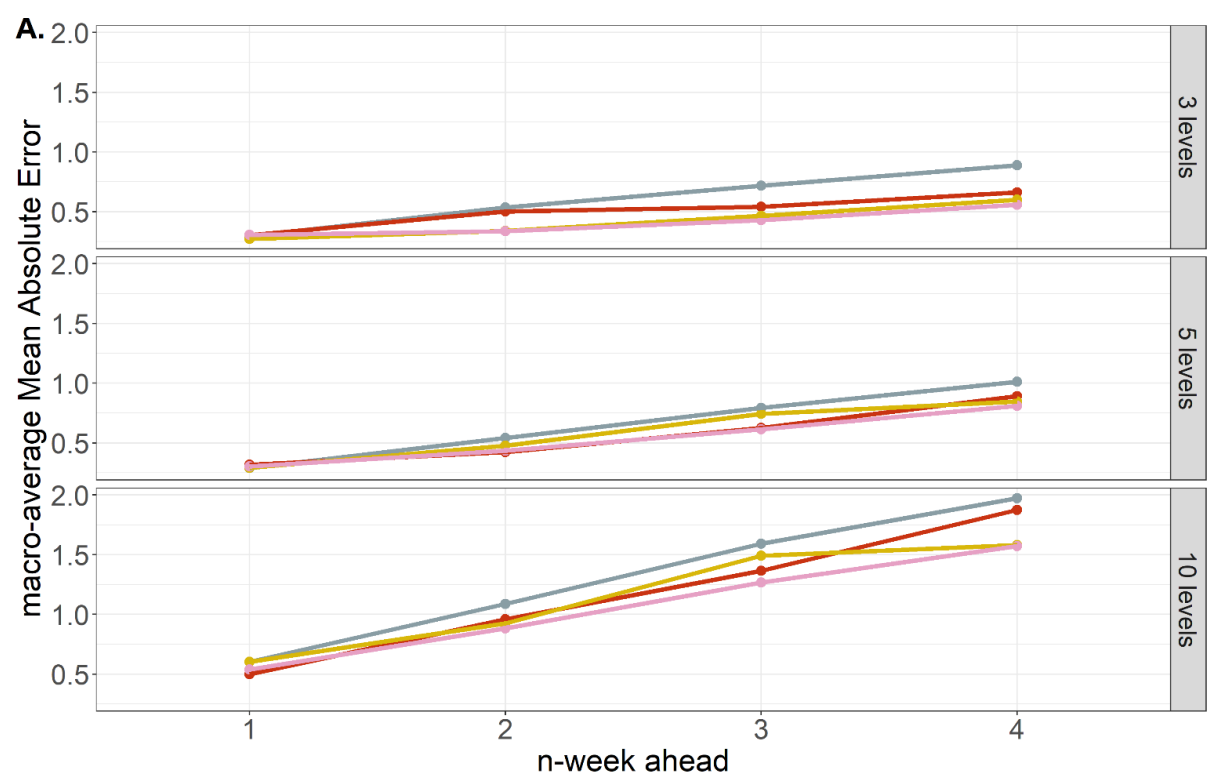
530

531

532

533 **S2 Figure. Epidemic curve of weekly hospitalisation by NHS regions in England from**
534 **19 March 2020 to 31 December 2022.** The left y-axis is the numerical number of weekly
535 new hospital admissions (red line), while the right y-axis is the ordinal weekly hospitalisation
536 level defined by the N-tile method (blue line) and the uniform method (yellow line). **A.** The
537 number of levels equals three. **B.** The number of levels equals five.

538



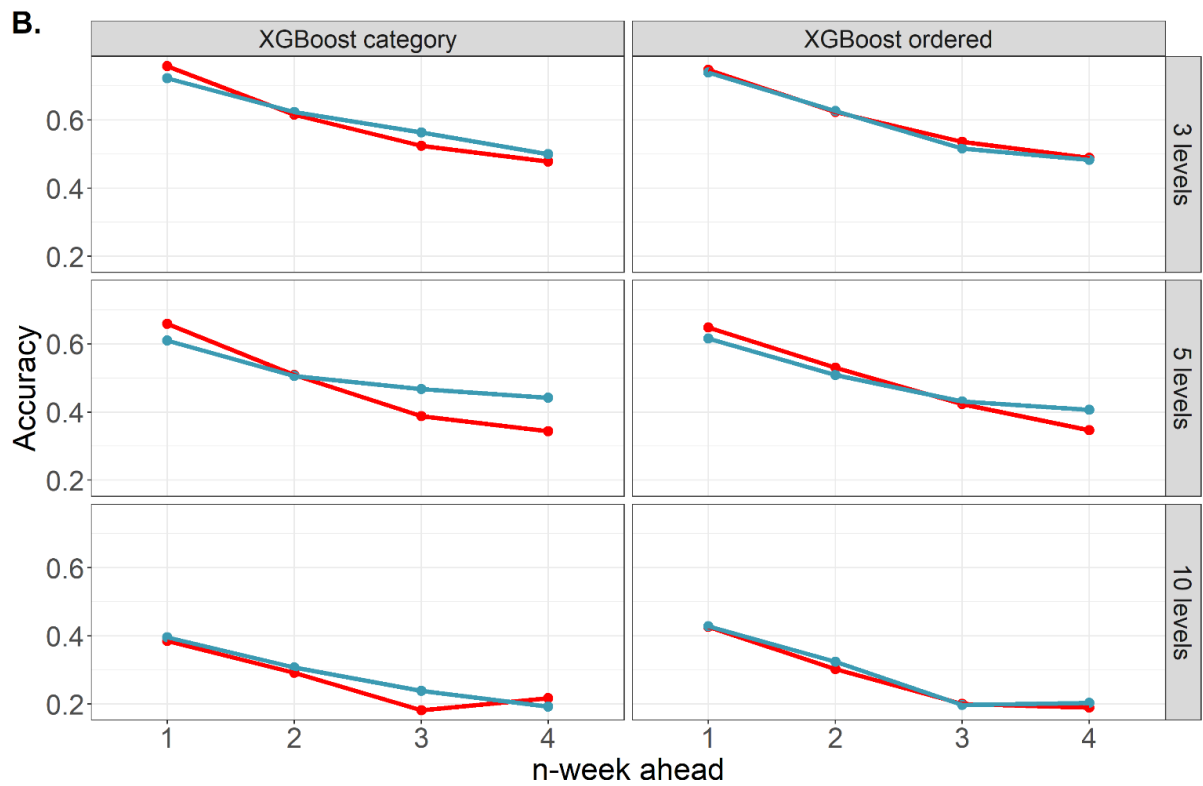
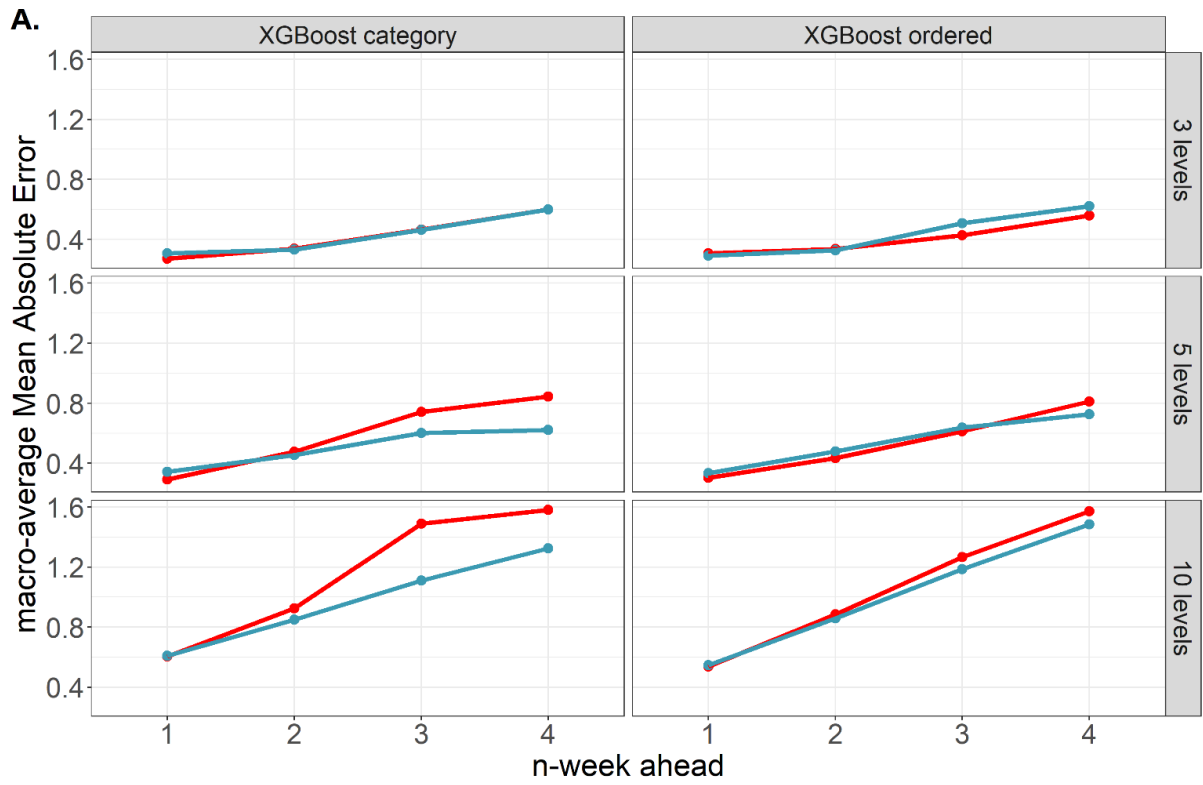
Model ● Null Model ● OLR ● XGBoost category ● XGBoost ordered

539

540 **S3 Figure. Model performance of predicting N-tile hospitalisation levels with only**
541 **epidemiological predictors. A.** mMAEs of the null model (grey line), ordered logistic
542 regression model (red line), the XGBoost category model (yellow line) and the XGBoost
543 model (pink line). **B.** Accuracy of the null model (grey line), ordered logistic regression model
544 (red line), the XGBoost category model (yellow line) and the XGBoost model (pink line).

545

546

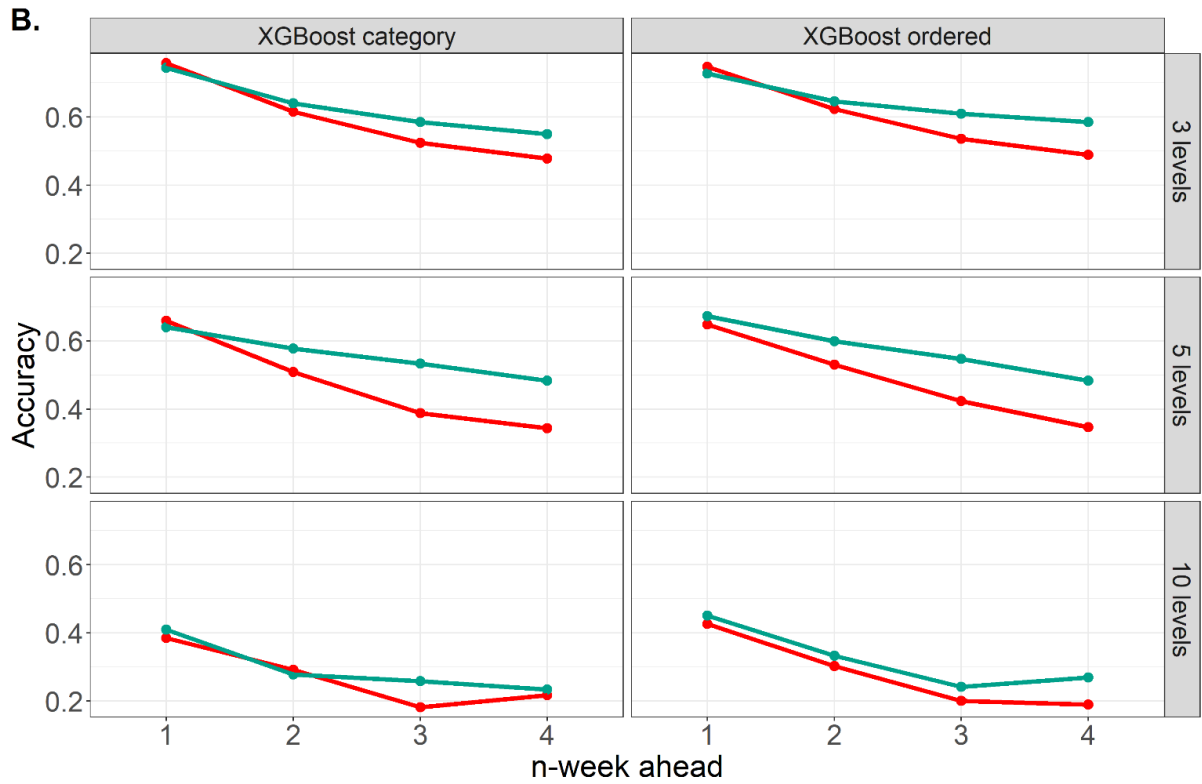
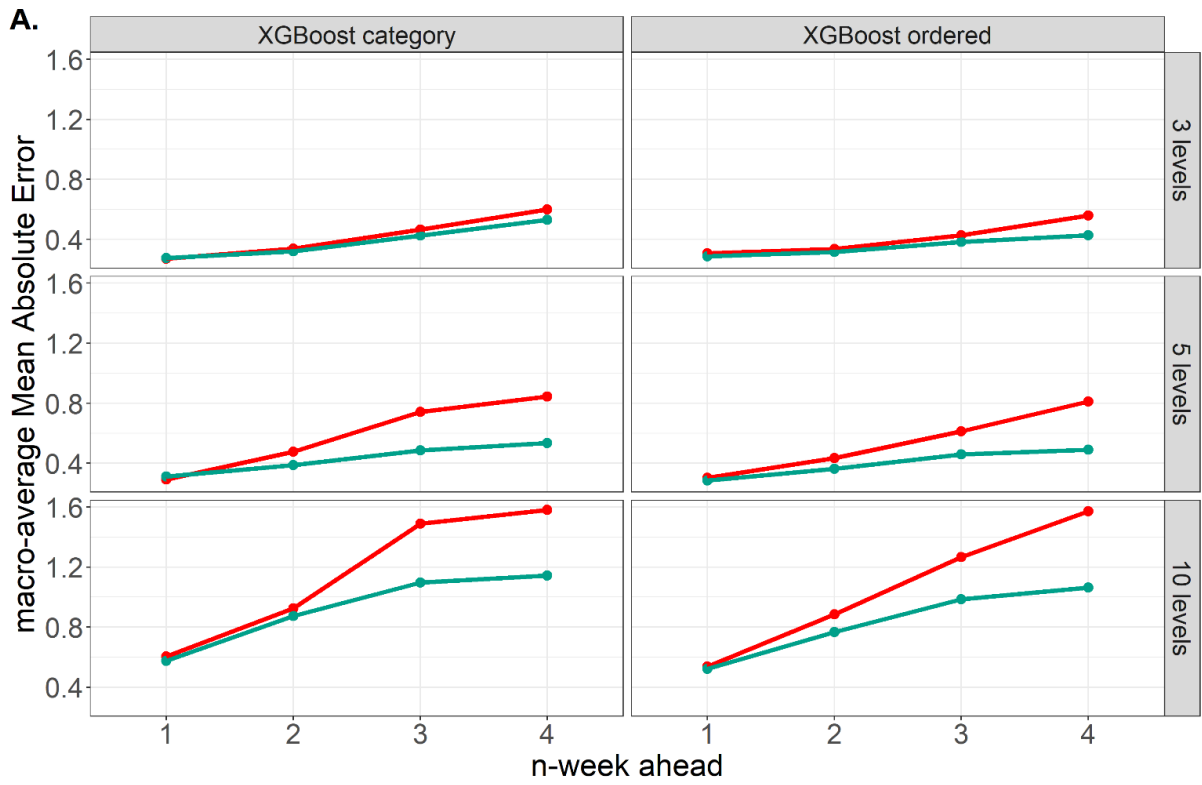


547

Data ◆ Epi* features ◆ Epi*+Weather features

548 **S4 Figure. Performance of the XGBoost models incorporated with epidemiological**
549 **and weather data, measured by macro-averaged Mean Absolute Error (mMAE) and**
550 **accuracy.** The overall mMAE and accuracy were averaged over seven NHS regions for
551 each prediction horizon (1- to 4-week ahead). **A.** mMAEs of the XGBoost models trained
552 with epidemiological and weather features (blue line) and epidemiological features (red line).
553 **B.** Accuracy of the XGBoost models trained with epidemiological and weather features (blue
554 line) and epidemiological features (red line).
555 *Epidemiological

556



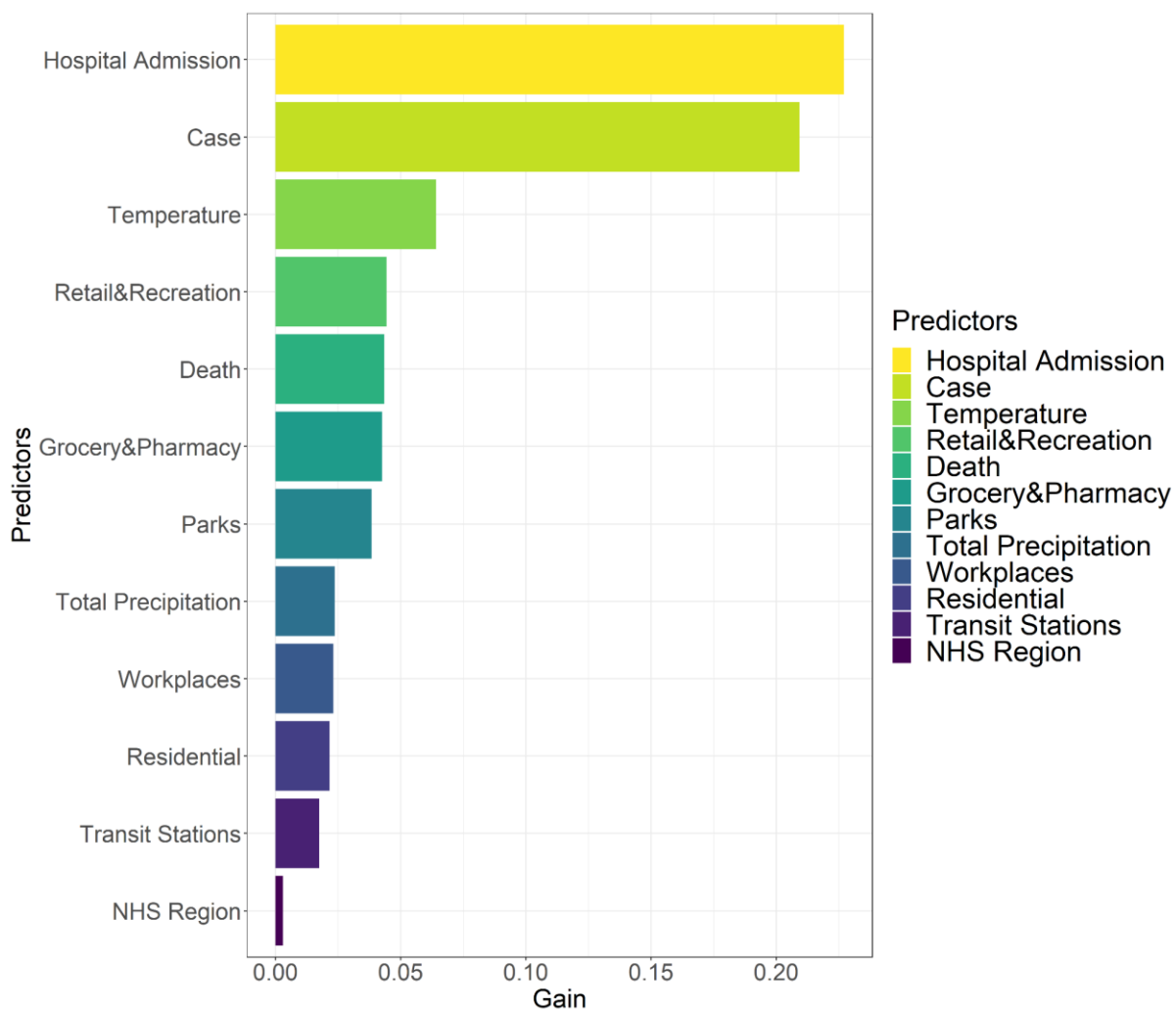
557

Data ● Epi* features ● Epi*+Mobility features

558 **S5 Figure. Performance of the XGBoost models incorporated with epidemiological**
559 **and mobility data, measured by macro-averaged Mean Absolute Error (mMAE) and**
560 **accuracy.** The overall mMAE and accuracy were averaged over seven NHS regions for
561 each prediction horizon (1- to 4-week ahead). **A.** mMAEs of the XGBoost models trained
562 with epidemiological and mobility features (green line) and epidemiological features (red
563 line). **B.** Accuracy of the XGBoost models trained with epidemiological and mobility features
564 (green line) and epidemiological features (red line).

565 *Epidemiological

566



567

568 **S6 Figure. The relative importance (Gain) of predictors used by the XGBoost ordered**
569 **model.**

570

571 Data availability

572 The source code and data used to produce the results and analyses presented in this
573 manuscript and supporting figures and tables are available on a Git repository:
574 https://github.com/VVVVivi/COVID_hosp_forecasting.git. Supporting figures and tables are
575 provided in the same GitHub repository as extended data.

576 Competing Interest

577 No competing interests were disclosed.

578 Acknowledgements

579 The authors acknowledge funding from the MRC Centre for Global Infectious Disease
580 Analysis (MR/R015600/1), jointly funded by the UK Medical Research Council (MRC) and
581 the UK Foreign, Commonwealth & Development Office (FCDO), under the MRC/FCDO
582 Concordat agreement, and also part of the EDCTP2 programme supported by the European
583 Union. S.R. acknowledges the support from Wellcome Trust Investigator Award (UK,
584 200861/Z/16/Z). KOK acknowledges funding from HMRF (INF-CUHK-1). RL acknowledges
585 funding from Nanjing Medical University Talents Start-up Grants (NMUR20220001).

586 Author Contribution

587 **Conceptualization:** Haowei Wang, Steven Riley

588 **Data curation:** Haowei Wang

589 **Formal analysis:** Haowei Wang

590 **Methodology:** Haowei Wang

591 **Software:** Haowei Wang

592 **Supervision:** Steven Riley

593 **Validation:** Haowei Wang

594 **Visualization:** Haowei Wang

595 **Writing – original draft:** Haowei Wang

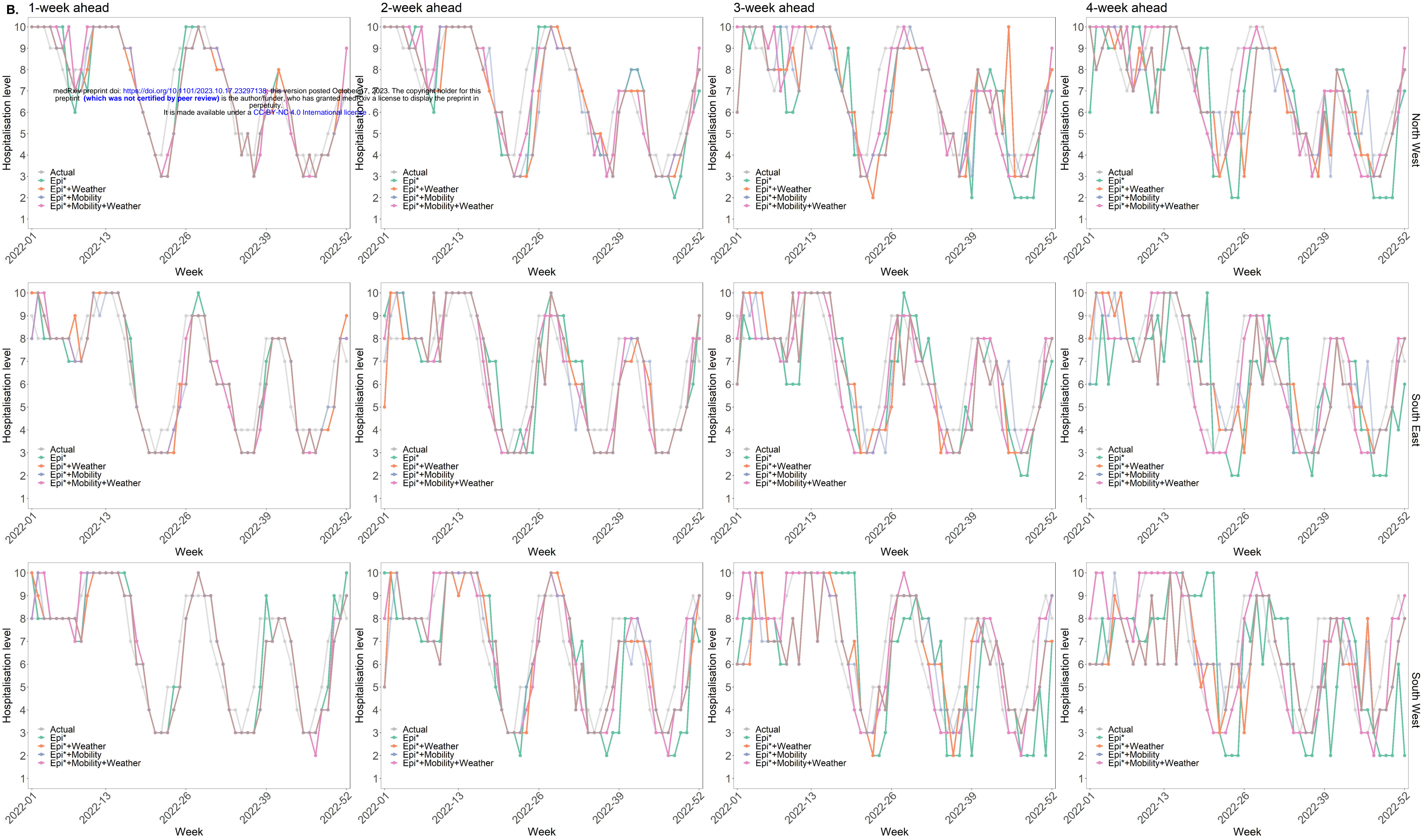
596 **Writing – review & editing:** Haowei Wang, Steven Riley, Kin On Kwok, Ruiyun Li

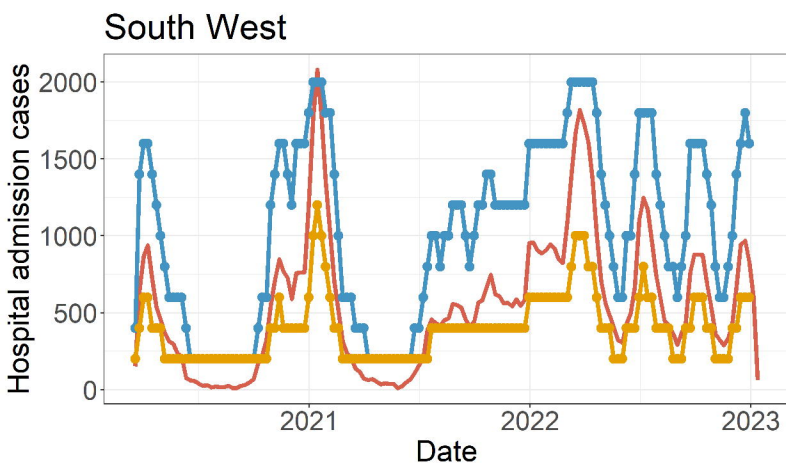
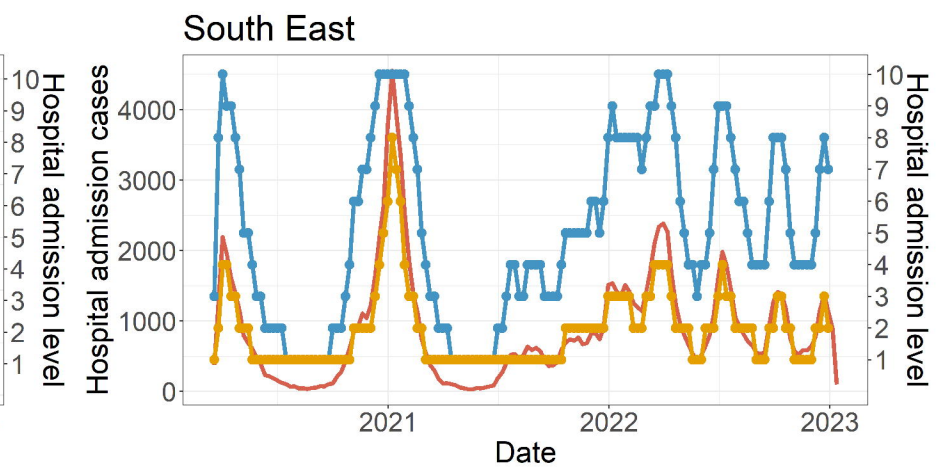
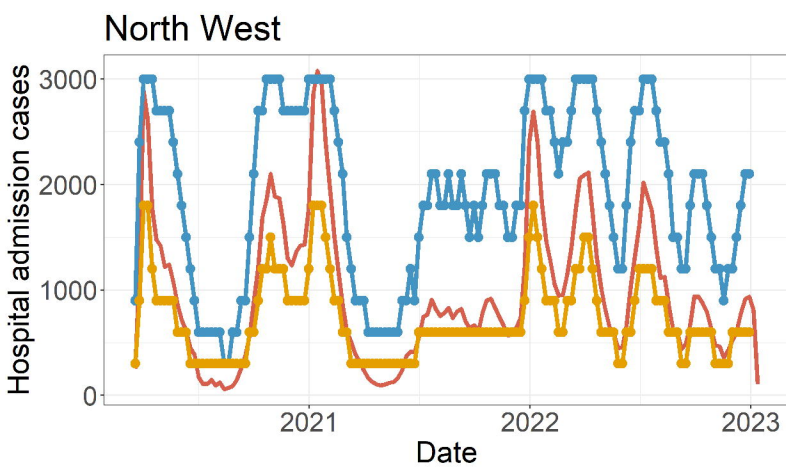
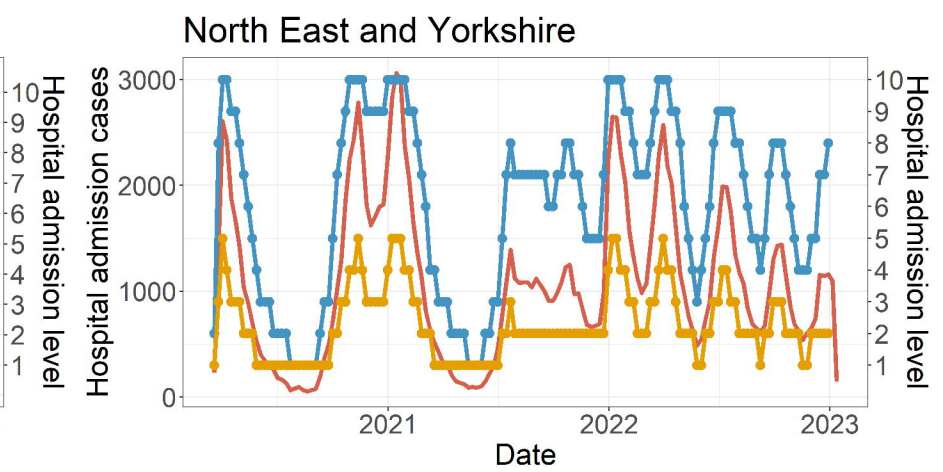
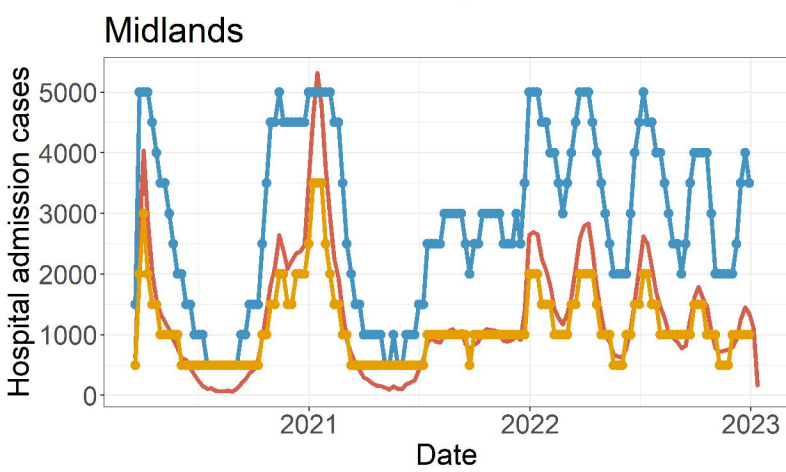
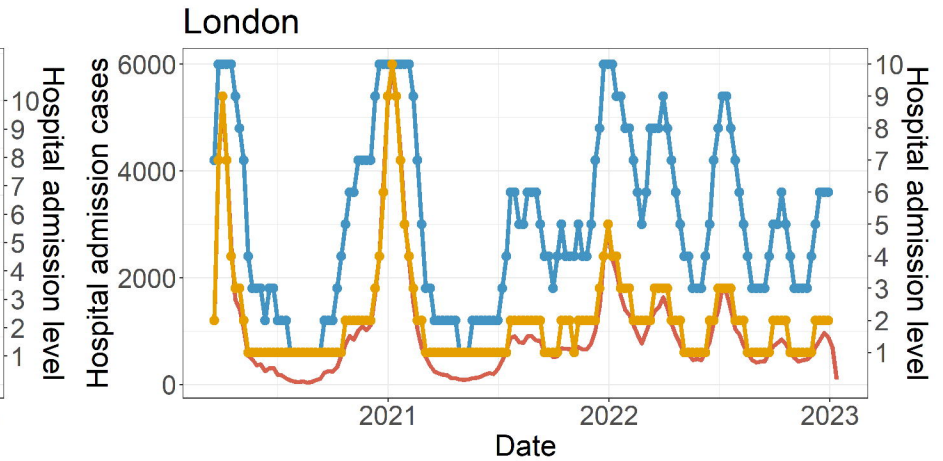
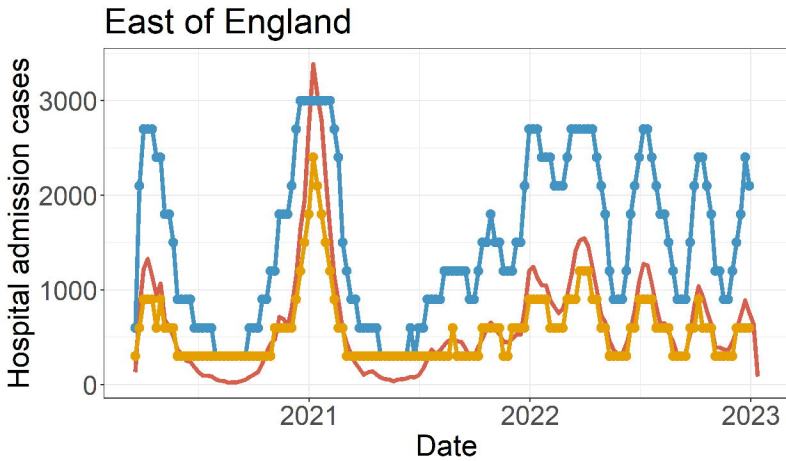
597 Reference

- 598 1. World Health Organization (WHO). WHO Coronavirus (COVID-19) Dashboard. 2020
599 [cited 11 Jan 2023]. Available: <https://covid19.who.int/>
- 600 2. Sarker S, Jamal L, Ahmed SF, Irtisam N. Robotics and artificial intelligence in
601 healthcare during COVID-19 pandemic: A systematic review. *Rob Auton Syst.*
602 2021;146: 103902. doi:10.1016/j.robot.2021.103902
- 603 3. Ilin C, Annan-Phan S, Tai XH, Mehra S, Hsiang S, Blumenstock JE. Public mobility data
604 enables COVID-19 forecasting and management at local and global scales. *Sci Rep.*
605 2021;11: 13531. doi:10.1038/s41598-021-92892-8
- 606 4. Ganslmeier M, Furceri D, Ostry JD. The impact of weather on COVID-19 pandemic. *Sci*
607 *Rep.* 2021;11: 22027. doi:10.1038/s41598-021-01189-3
- 608 5. McClymont H, Hu W. Weather Variability and COVID-19 Transmission: A Review of
609 Recent Research. *Int J Environ Res Public Health.* 2021;18.
610 doi:10.3390/ijerph18020396
- 611 6. Wu Y, Jing W, Liu J, Ma Q, Yuan J, Wang Y, et al. Effects of temperature and humidity
612 on the daily new cases and new deaths of COVID-19 in 166 countries. *Sci Total*
613 *Environ.* 2020;729: 139051. doi:10.1016/j.scitotenv.2020.139051
- 614 7. d'Albis H, Coulibaly D, Roumagnac A, de Carvalho Filho E, Bertrand R. Quantification of
615 the effects of climatic conditions on French hospital admissions and deaths induced by
616 SARS-CoV-2. *Sci Rep.* 2021;11: 21812. doi:10.1038/s41598-021-01392-2
- 617 8. Paireau J, Andronico A, Hozé N, Layan M, Crépey P, Roumagnac A, et al. An ensemble
618 model based on early predictors to forecast COVID-19 health care demand in France.
619 *Proc Natl Acad Sci U S A.* 2022;119: e2103302119. doi:10.1073/pnas.2103302119
- 620 9. Moran KR, Fairchild G, Generous N, Hickmann K, Osthus D, Priedhorsky R, et al.
621 Epidemic Forecasting is Messier Than Weather Forecasting: The Role of Human
622 Behavior and Internet Data Streams in Epidemic Forecast. *J Infect Dis.* 2016;214:
623 S404–S408. doi:10.1093/infdis/jiw375
- 624 10. Ainslie KEC, Walters CE, Fu H, Bhatia S, Wang H, Xi X, et al. Evidence of initial
625 success for China exiting COVID-19 social distancing policy after achieving
626 containment. *Wellcome Open Res.* 2020;5: 81. doi:10.12688/wellcomeopenres.15843.2
- 627 11. Klein B, LaRock T, McCabe S, Torres L, Friedland L, Kos M, et al. Characterizing
628 collective physical distancing in the U.S. during the first nine months of the COVID-19
629 pandemic. *arXiv [physics.soc-ph]*. 2022. Available: <http://arxiv.org/abs/2212.08873>
- 630 12. Wang H, Kwok KO, Riley S. Forecasting influenza incidence as an ordinal variable
631 using machine learning. *medRxiv.* 2023. doi:10.1101/2023.02.09.23285705
- 632 13. England Summary. [cited 13 Jan 2023]. Available: <https://coronavirus.data.gov.uk/>
- 633 14. Office for National Statistics. Estimates of the population for the UK, England, Wales,
634 Scotland and Northern Ireland. Office for National Statistics; 2022. Available:
635 [https://www.ons.gov.uk/peoplepopulationandcommunity/populationandmigration/populat](https://www.ons.gov.uk/peoplepopulationandcommunity/populationandmigration/populationestimates/datasets/populationestimatesforukenglandandwalesscotlandandnorthernireland)
636 [ionestimates/datasets/populationestimatesforukenglandandwalesscotlandandnorthernir](https://www.ons.gov.uk/peoplepopulationandcommunity/populationandmigration/populationestimates/datasets/populationestimatesforukenglandandwalesscotlandandnorthernireland)
637 [eland](https://www.ons.gov.uk/peoplepopulationandcommunity/populationandmigration/populationestimates/datasets/populationestimatesforukenglandandwalesscotlandandnorthernireland)

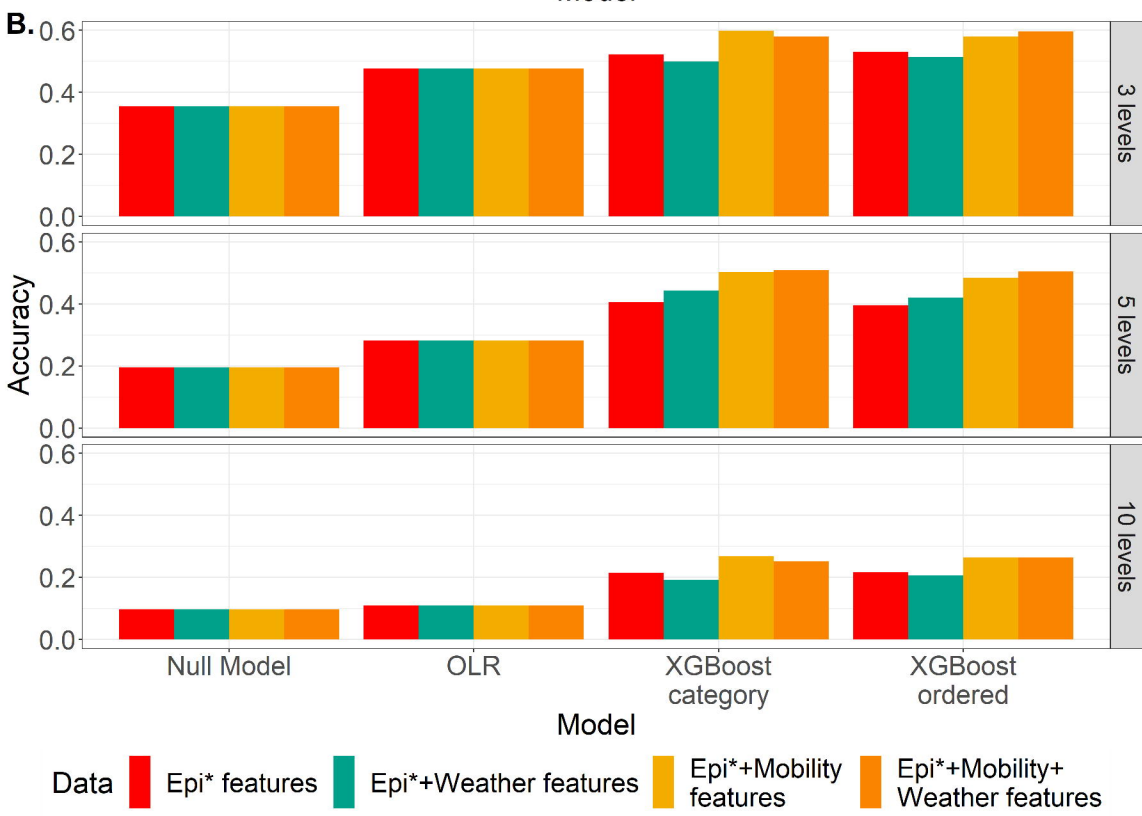
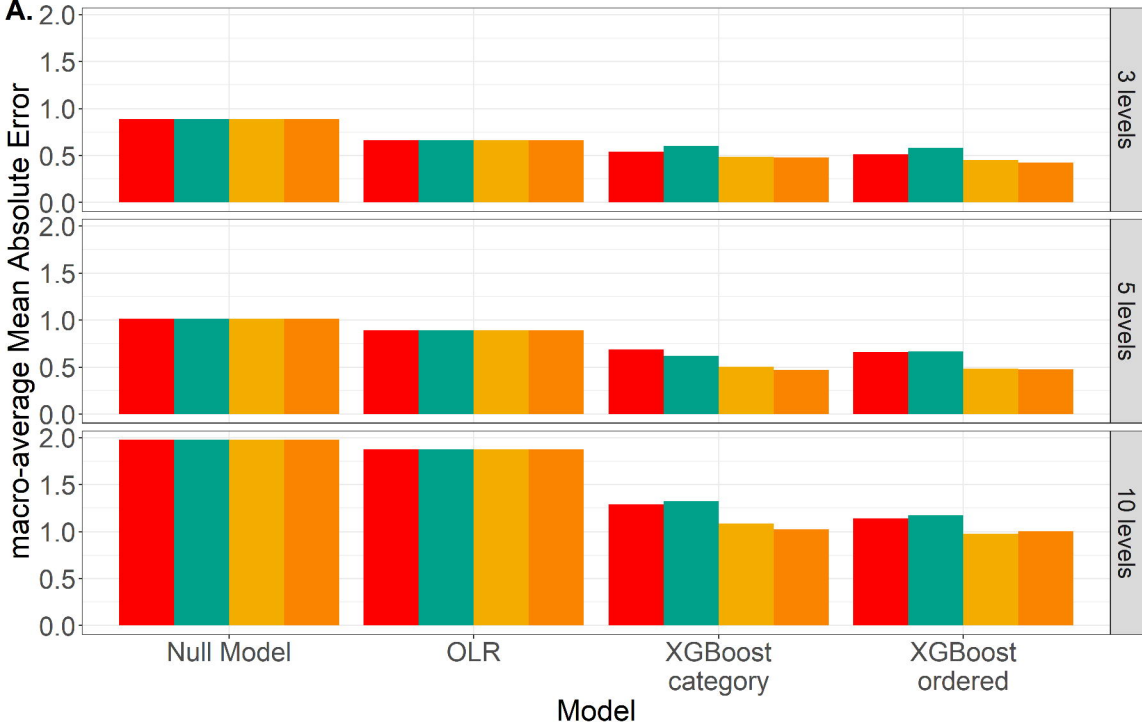
- 638 15. Google. COVID-19 Community Mobility Reports. 2020. Available:
639 <https://www.google.com/covid19/mobility/>
- 640 16. Data Science Campus. google-mobility-reports-data: Archive of data extracted from the
641 google community mobility reports. Github; 2020. Available:
642 <https://github.com/datasciencecampus/google-mobility-reports-data>
- 643 17. Hersbach H, Bell B, Berrisford P, Hirahara S, Horányi A, Muñoz-Sabater J, et al. The
644 ERA5 global reanalysis. *Quart J Roy Meteor Soc.* 2020;146: 1999–2049.
645 doi:10.1002/qj.3803
- 646 18. Frank E, Hall M. A Simple Approach to Ordinal Classification. *Machine Learning: ECML*
647 2001. Berlin, Heidelberg: Springer Berlin Heidelberg; 2001. pp. 145–156. doi:10.1007/3-
648 540-44795-4_13
- 649 19. Parry S. 91_ordlogistic.pdf. 2016. Available: [https://cscu.cornell.edu/wp-](https://cscu.cornell.edu/wp-content/uploads/91_ordlogistic.pdf)
650 [content/uploads/91_ordlogistic.pdf](https://cscu.cornell.edu/wp-content/uploads/91_ordlogistic.pdf)
- 651 20. Badr HS, Du H, Marshall M, Dong E, Squire MM, Gardner LM. Association between
652 mobility patterns and COVID-19 transmission in the USA: a mathematical modelling
653 study. *Lancet Infect Dis.* 2020;20: 1247–1254. doi:10.1016/S1473-3099(20)30553-3
- 654 21. Kraemer MUG, Yang C-H, Gutierrez B, Wu C-H, Klein B, Pigott DM, et al. The effect of
655 human mobility and control measures on the COVID-19 epidemic in China. *Science.*
656 2020;368: 493–497. doi:10.1126/science.abb4218
- 657 22. Klein B, Zenteno AC, Joseph D, Zahedi M, Hu M, Copenhaver MS, et al. Forecasting
658 hospital-level COVID-19 admissions using real-time mobility data. *Commun Med.*
659 2023;3: 25. doi:10.1038/s43856-023-00253-5
- 660 23. Kwok KO, Wei WI, Huang Y, Kam KM, Chan EYY, Riley S, et al. Evolving
661 Epidemiological Characteristics of COVID-19 in Hong Kong From January to August
662 2020: Retrospective Study. *J Med Internet Res.* 2021;23: e26645. doi:10.2196/26645
- 663 24. Xiong C, Hu S, Yang M, Luo W, Zhang L. Mobile device data reveal the dynamics in a
664 positive relationship between human mobility and COVID-19 infections. *Proc Natl Acad*
665 *Sci U S A.* 2020;117: 27087–27089. doi:10.1073/pnas.2010836117
- 666 25. Salje H, Tran Kiem C, Lefrancq N, Courtejoie N, Bosetti P, Paireau J, et al. Estimating
667 the burden of SARS-CoV-2 in France. *Science.* 2020;369: 208–211.
668 doi:10.1126/science.abc3517
- 669 26. Davies NG, Klepac P, Liu Y, Prem K, Jit M, Eggo RM. Age-dependent effects in the
670 transmission and control of COVID-19 epidemics. *Nat Med.* 2020;26: 1205–1211.
671 doi:10.1038/s41591-020-0962-9
- 672 27. Walker PGT, Whittaker C, Watson OJ, Baguelin M, Winskill P, Hamlet A, et al. The
673 impact of COVID-19 and strategies for mitigation and suppression in low- and middle-
674 income countries. *Science.* 2020;369: 413–422. doi:10.1126/science.abc0035
- 675 28. Wilder-Smith A, Freedman DO. Isolation, quarantine, social distancing and community
676 containment: pivotal role for old-style public health measures in the novel coronavirus
677 (2019-nCoV) outbreak. *J Travel Med.* 2020;27. doi:10.1093/jtm/taaa020
- 678 29. Lurie N, Saville M, Hatchett R, Halton J. Developing Covid-19 Vaccines at Pandemic
679 Speed. *N Engl J Med.* 2020;382: 1969–1973. doi:10.1056/NEJMp2005630

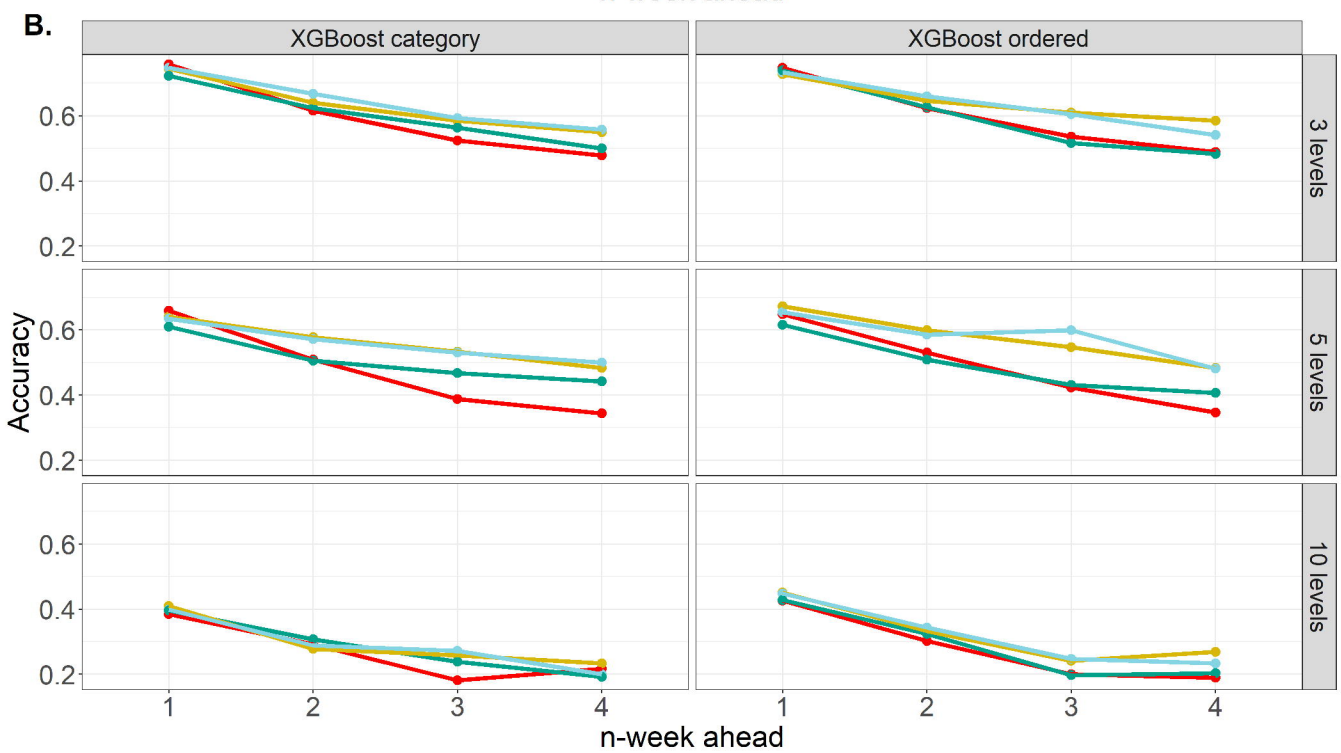
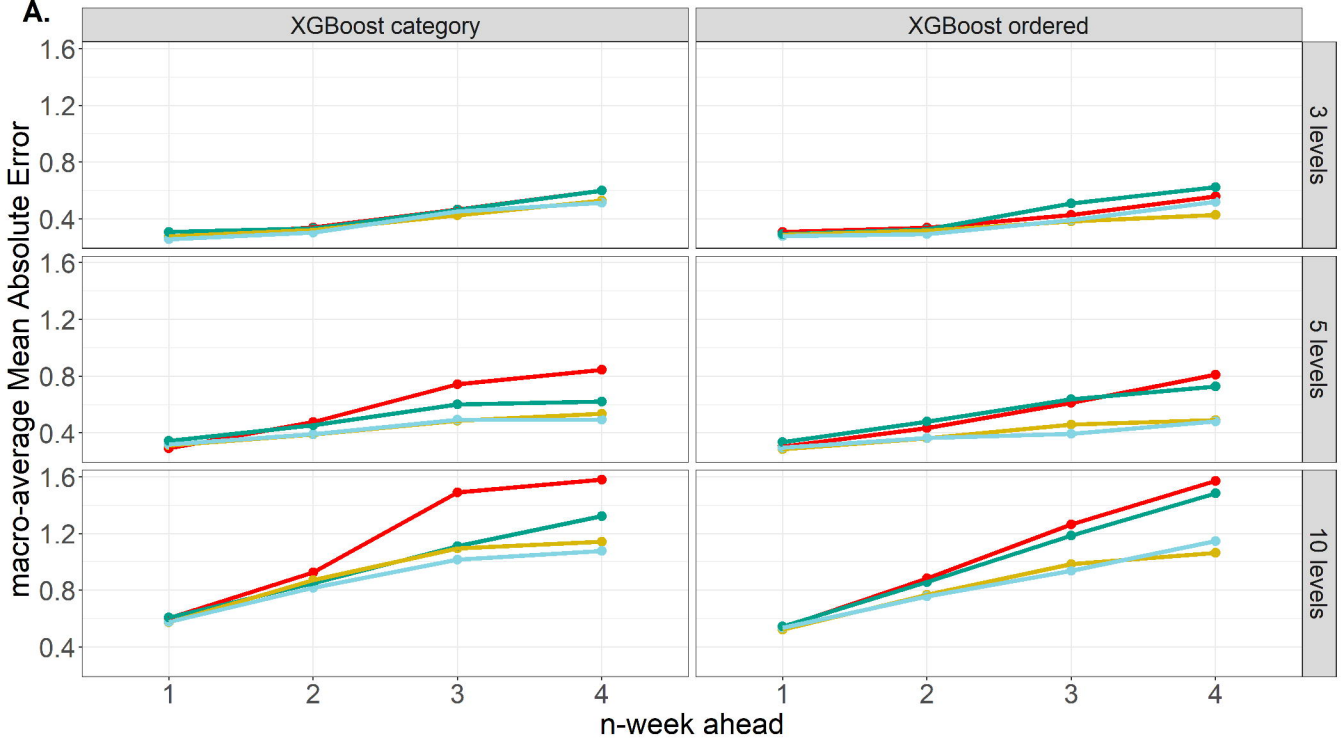
- 680 30. Haug N, Geyrhofer L, Londei A, Dervic E, Desvars-Larrive A, Loreto V, et al. Ranking
681 the effectiveness of worldwide COVID-19 government interventions. *Nature Human*
682 *Behaviour*. 2020;4: 1303–1312. doi:10.1038/s41562-020-01009-0
- 683 31. Flaxman S, Mishra S, Gandy A, Unwin HJT, Mellan TA, Coupland H, et al. Estimating
684 the effects of non-pharmaceutical interventions on COVID-19 in Europe. *Nature*.
685 2020;584: 257–261. doi:10.1038/s41586-020-2405-7
- 686



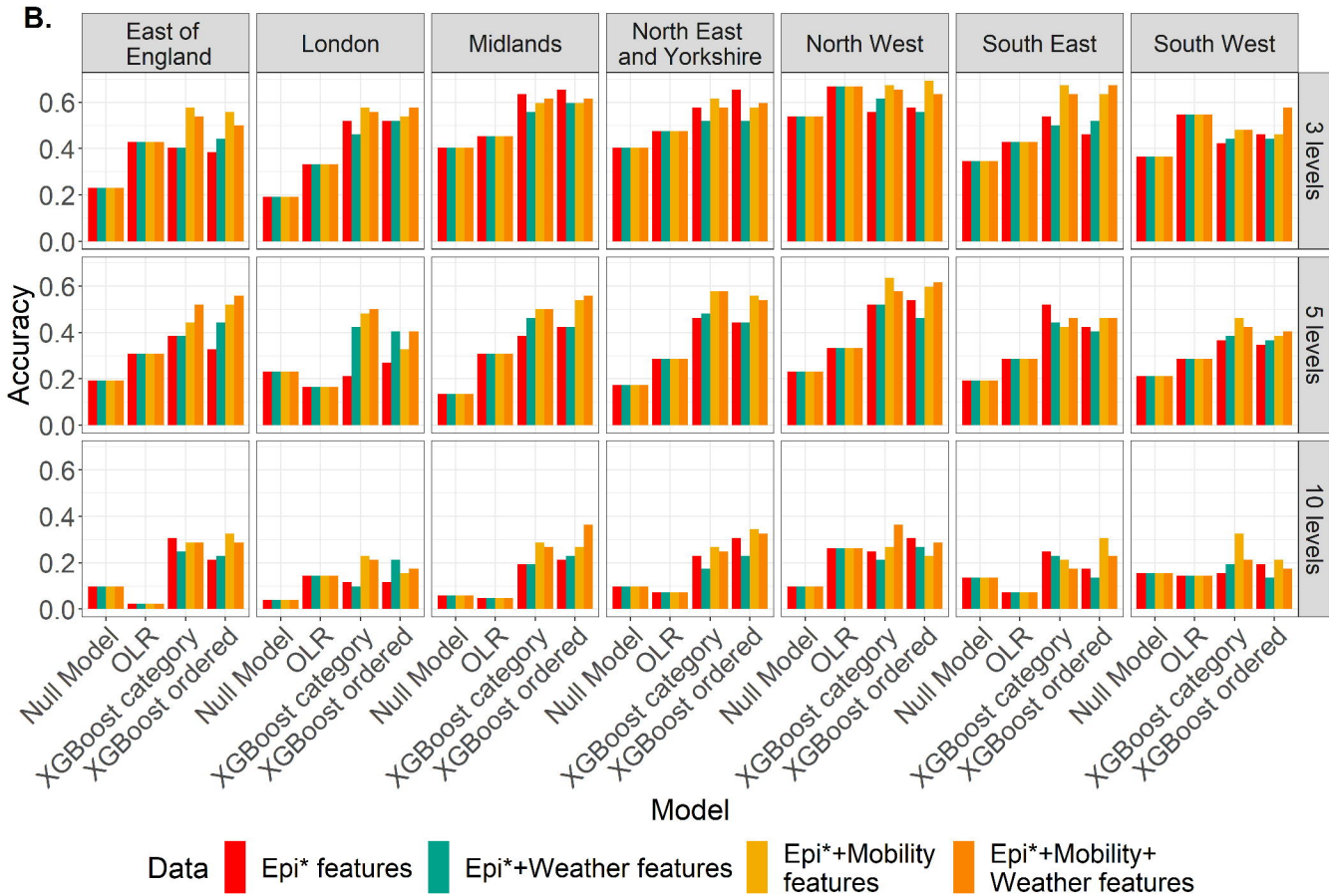
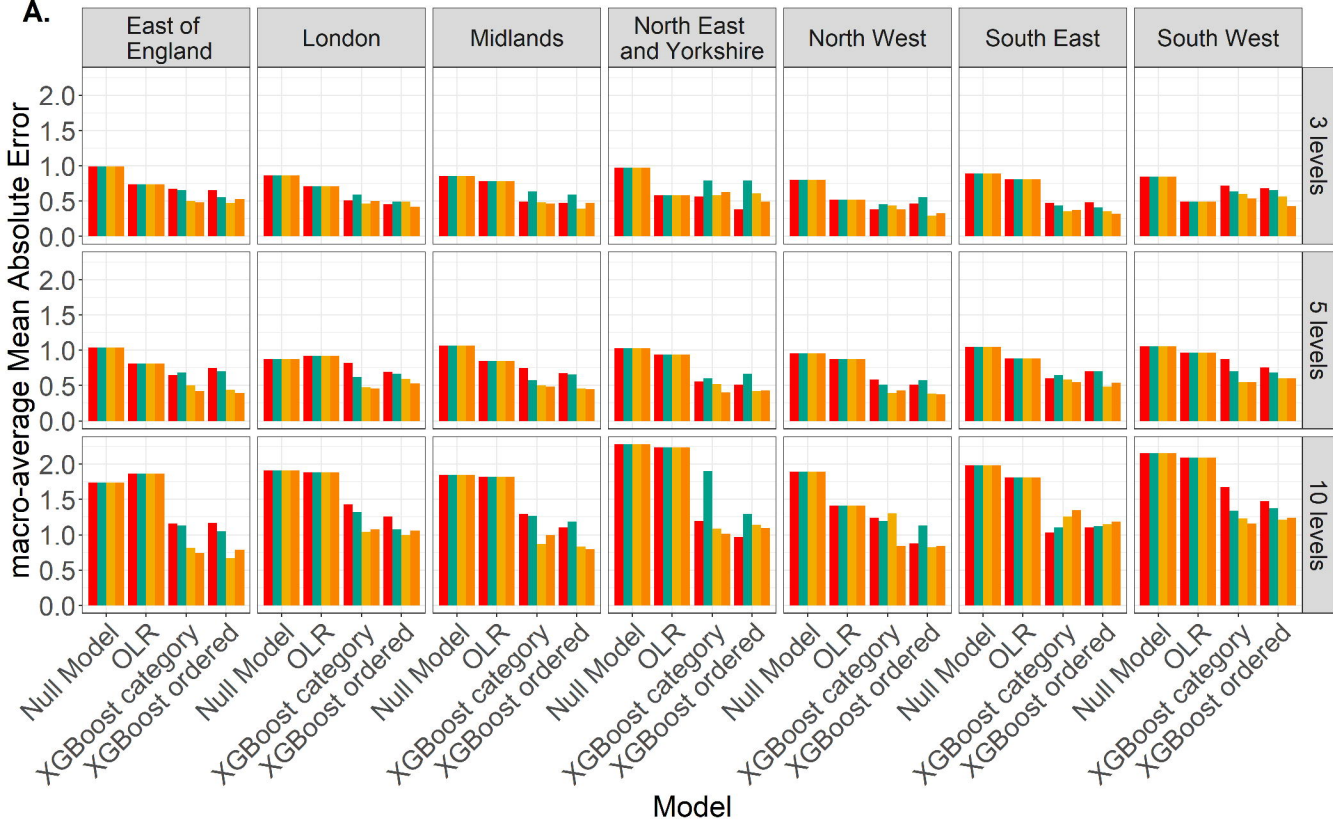


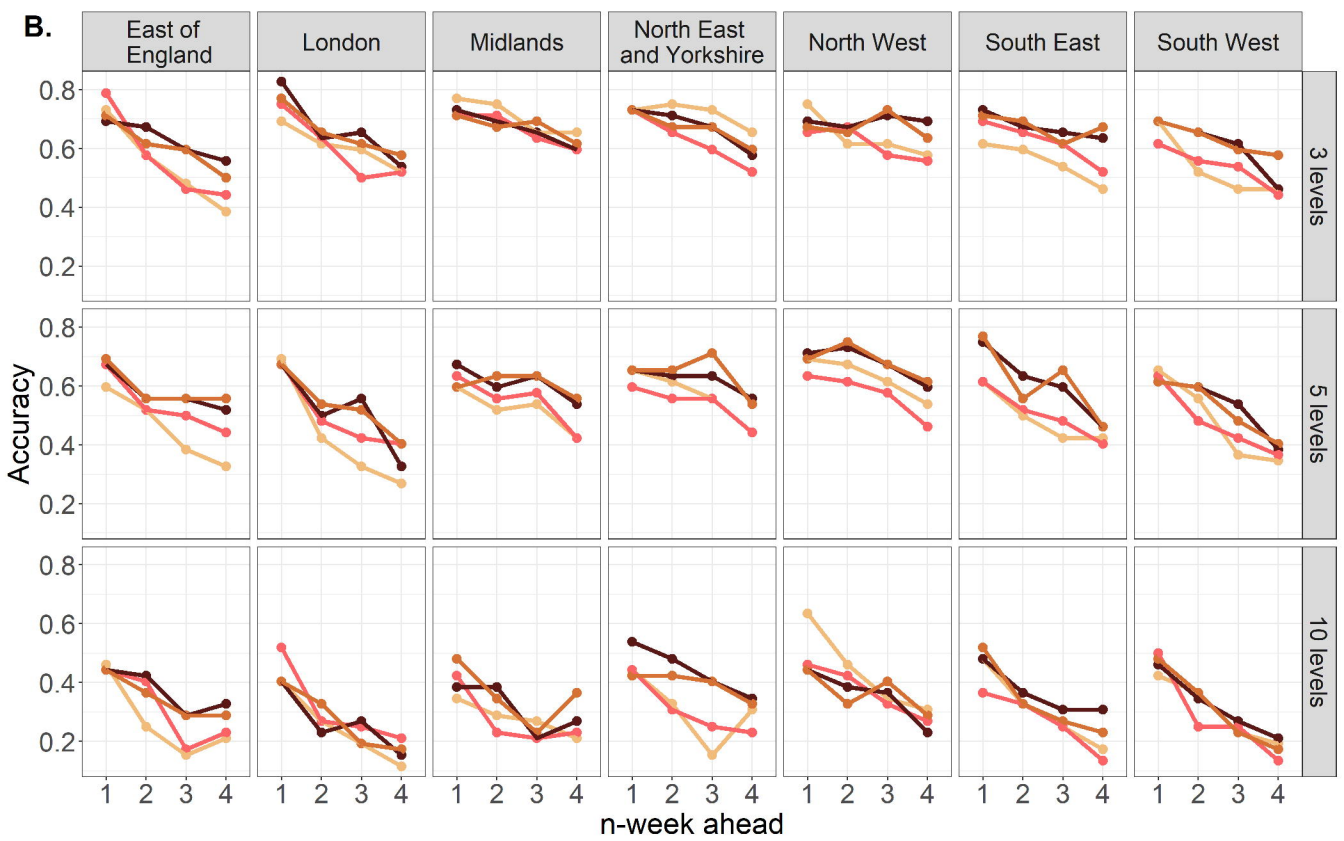
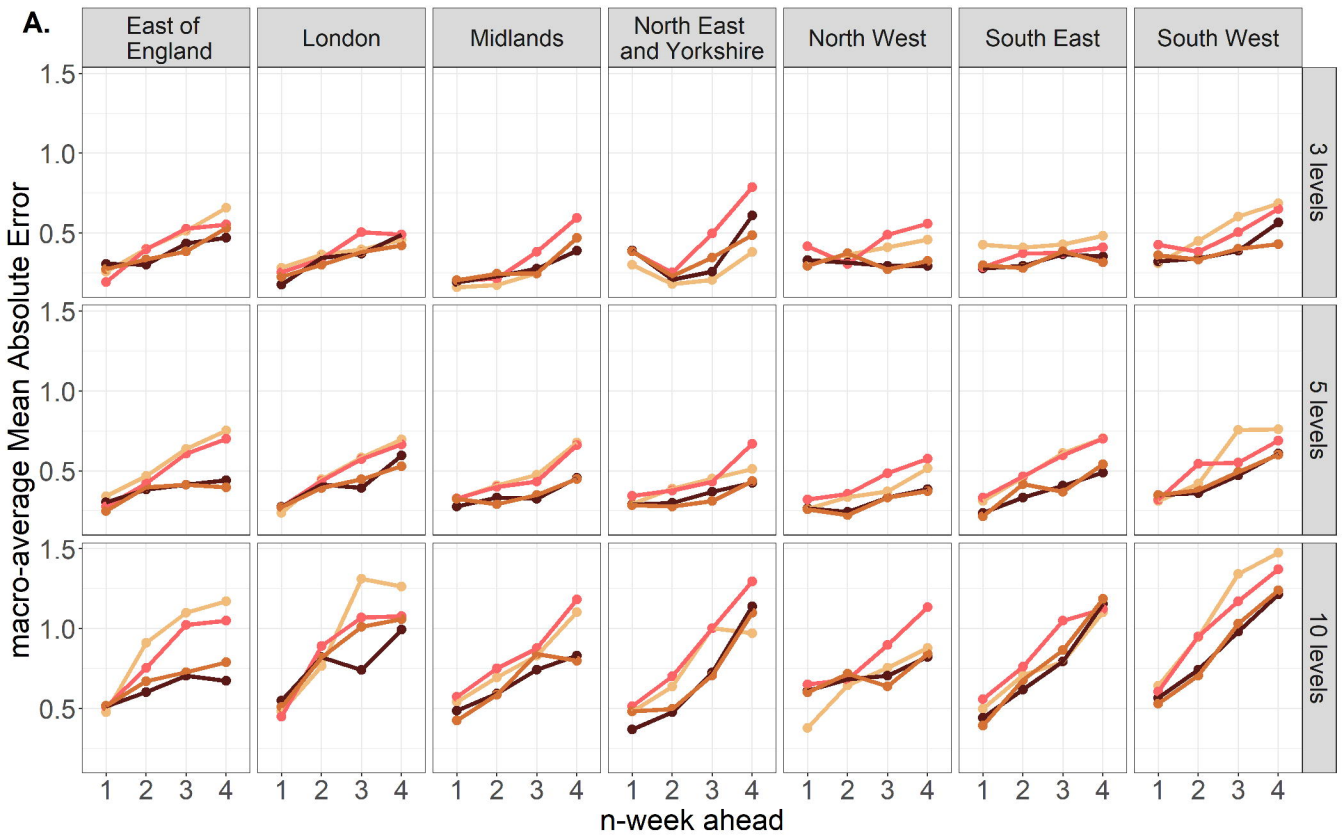
Hospitalisation — Hospital admission cases — Hospital admission level (n-tile) — Hospital admission level (uniform)





Data ● Epi* features ● Epi*+Weather features ● Epi*+Mobility features ● Epi*+Mobility+Weather features





Data — Epi* features — Epi*+Weather features — Epi*+Mobility features — Epi*+Mobility+Weather features

